2022-12-01

Inhibiting C-C Chemokine Receptor 7 Activation Of T-Cell Acute Lymphoblastic Leukemia By A Ccl19/macrophage Inflammatory Protein-3β Antagonist

Angel Torres
University of Texas at El Paso

INHIBITING C-C CHEMOKINE RECEPTOR 7 ACTIVATION OF T-CELL ACUTE LYMPHOBLASTIC LEUKEMIA BY A CCL19/MACROPHAGE INFLAMMATORY PROTEIN-3β ANTAGONIST

ANGEL TORRES

Master's Program in Biological Sciences

APPROVED:

Charlotte M. Vines, Ph.D., Chair

Hugues Ouellet, Ph.D.

Colin A. Bill, Ph.D.

Eva M. Moya, Ph.D.

Stephen L. Crites, Jr., Ph.D.
Dean of the Graduate School

INHIBITING C-C CHEMOKINE RECEPTOR 7 ACTIVATION OF T-CELL ACUTE LYMPHOBLASTIC LEUKEMIA BY A CCL19/MACROPHAGE INFLAMMATORY PROTEIN-3β ANTAGONIST

by

ANGEL TORRES, B.Sc.

THESIS

Presented to the Faculty of the Graduate School of

The University of Texas at El Paso

in Partial Fulfillment of the

requirements for

the Degree of

MASTER OF SCIENCE

Department of Biological Sciences

THE UNIVERSITY OF TEXAS AT EL PASO

December 2022

Abstract

The binding of C-C Chemokine Ligand 19 (CCL19) to C-C chemokine receptor 7 (CCR7) receptor has been linked to T-cell activation, tolerance, and inflammation. CCR7 is a member of the chemotactic cytokine family, essential in the development of T cells and regulatory processes such as immune-cell trafficking. This is accompanied by chemokine ligand concentration and time-dependent internalization, which is efficiently promoted by CCL19. A novel N-terminal truncation of CCL19 has been previously developed as an antagonist observed to impede induced chemotaxis and calcium mobilization in mouse primary immune cells. The current antagonist has suggested a key role of CCL198-83 in respect to allogeneic immune response. This antagonist was tested in human leukemic T-cells expressing the CCR7 receptor and was found to be effective in inhibition of chemotaxis and inhibiting receptor internalization in these cells. However, the production of the antagonist CCL19(8-83) is tied to an expensive technique not sustainable in upscaled productions. A more cost-effective production of antagonists is necessary to further understand the role of antagonizing CCR7 with CCL198-83. For instance, T-cell acute lymphoblastic leukemia (T-ALL) an aggressive hematologic cancer is linked to the CCR7 adhesion to its ligand CCL19 and is involved in chronic leukemia and its relapse. Further understanding of mechanisms of action and responses of CCR7 and CCL19 ligation is an important research subject for both biological and pathological areas. The challenges in producing functional chemokines are linked to improper folding of the chemokines. In this study, we attempted to produce a functional folded chemokine. Presently, chemical synthesis and heterologous expression systems in E. coli are initially unfolded, unoxidized and nonfunctional. Since refolded synthetic or recombinant chemokines are desired, a process of cysteine oxidation is necessary. Following current literature, we suggest the use of a SUMO fusion protein for chemokine production that is

more cost effective. We have developed a potential effective system to produce CCL198-83 antagonist that can improve the current data on CCR7 binding that could have a potential impact as treatment target for different hematological diseases, such as T-ALL.

Table of Contents

List of Tables

List of Figures

Chapter 1: Introduction

1.1 G Protein-Coupled Receptors

G protein-coupled receptors (GPCRs) have structural diversity. The amino terminal domain localizes in the extracellular portion of the receptor along the three extracellular loops and the extracellular portions of the transmembrane regions make-up the extracellular domain. This extracellular portion is the one that diversifies the most between GPCRs because the different types of ligands will bind to this portion. The conserved portion in GPCRs is the intracellular domain made up of three intracellular loops along of the intracellular portions of the transmembrane regions. The reason why this portion is conserved is because to it the heterotrimeric G proteins and other signaling molecules will bind to it. Whereas a small portion of GPCRs can be activated without its ligand molecules, the general model is that GPCRs can exist in two states, active and inactive. There is a consensus of activation mechanism among the GPCRs to which mechanism has been elucidated and their conformational changes, such as Rhodopsin, AA_{2A}AR, and β_2-AR receptors.

The secondary signaling molecules are the heterotrimeric G-proteins. They are made up of three different subunits bound together creating the alpha, beta, and gamma complex (G-$G_{\alpha}\beta\gamma$) (Figure 1.1.1) [1]. These subunits can be in two states: on and off. In the activated state the subunits are not all bound together instead they are dissociated into two separate portions, the α subunit and the βγ dimer. In the active state the α subunit has GTP bound to it resulting in a conformational change that cannot interact with the βγ complex. GTP is immediately hydrolyzed to GDP causing the inactive state of the G protein by reassembling α subunit to βγ creating once again the αβγ trimer. The G protein is a cytoplasmic protein attached to the cytoplasmic face of the plasma membrane by lipid moieties 14-16 saturated hydrocarbons chains, attached to the α and γ subunits.

The phospholipid bilayer facing the cytoplasm is extremely hydrophobic, making the ideal conditions for the hydrophobic α subunit to interact with it, moving away from water molecules and anchoring itself to the phospholipid bilayer in a thermodynamically favorable state. Under the 14 (myristoyl)-16(palmitoyl) carboxylic acid, consequently the α subunit rests underneath close to the N-termini, such as $G_{\alpha\,i1}$. The later alpha subunit increases its affinity to adenylyl cyclase Gβγ subunits, relatively more than supporting membrane interaction. The γ subunit also has a lipid chain, geranylgeranyl, and farnesyl (isoprene groups). Once again as it is extremely hydrophobic chain it ends up anchoring the γ subunit to the inner part of the phospholipid bilayer. There are many heterotrimeric G proteins and a modest number of α, β and γ isoforms. There are four classes of Gα subunits within the family: s, i, q/11 and 12/13. The first class is for the activation of adenylyl cyclases, the second one for inhibition of certain adenylyl cyclase isoforms, the third one for phospholipases β activation and finally the last one is necessary for the activation of GEFs. During splicing the subunits can form different isomers of alpha subunits. Pre-mRNA can be spliced in different isoforms such as $G_{\alpha s}$, and $G_{\alpha olf}$, that can be found at the olfactory epithelium, just to name a few. $G_{\alpha/}\emptyset$, has 8 members, G_{i1}, G_{i2}, G_{i3} (3 genes), and other Gα isoforms that correspond to the transducing of signals within photoreceptors in the eye or gustatory system. In total there are 16 genes for α subunits. The known mechanism of $G_{\alpha\,i}$ corresponds with the inhibition of cAMP dependent pathways by inhibiting adenylyl cyclase, in contrast it activates tyrosine kinase c-Src. $G_{\alpha\,i1}$ interacts with a variety of proteins like C-C motif chemokine receptor 7 (CCR7) and the receptor's ligands CCL19/CCL21 which leads to the homeostasis of T-cells, antigen presenting dendritic cells (DCs), and B cells.

The membrane bound receptor GPCR has a site in the ECM (extracellular matrix) where a ligand can bind to it. The portion of the receptor inside of the cell can bind to the G protein. G

proteins exist as two different classes: small monomeric GTPases, or as complex consisting of heterotrimeric G proteins or large GTP binding complexes. On its own the beta and gamma subunits can also make a beta-gamma complex (βγ). The heterotrimeric G protein is bound to the cell membrane via covalently attached fatty acids. The G-protein contains a bound guanine nucleotide. In the inactive state the G protein trimer has a bound molecule of GDP. The chemokine binding of chemokines such as CCL19 and CCL21 triggers the association of the G protein with the receptor by exchanging GDP (guanosine diphosphate) for GTP (guanosine triphosphate). In the active state both dissociated molecules Gα and βγ molecules can serve as secondary messengers activating other intracellular molecules and signaling pathways.

CCR7 is essential in the regulation of immune cell trafficking a GPCR with seven transmembrane spanning alpha helices[2]. CCR7 is a key regulator that directs homeostatic lymphocytes to secondary lymphoid organs which is achieved by binding to its ligands CCL19/CCL21 (Figure 1.1.3)[3]. It is expressed on double negative and single-positive thymocytes, including naive T cells, central memory T cells, regulatory T cells, naive B cells, semi-mature/mature dendritic cells (DCs) and natural killer (NK) cells, and a small percentage of tumor cells[4–7]. CCR7 mediated signaling controls the relocation of DCs into the lymphoid organs, such as the spleen which culminates in T cell activation. As this receptor's importance in the immune system is elucidated, it is well understood that it has key roles in development and regulation of immunity and tolerance. As a chemokine receptor it regulates chemotaxis (MAPK pathway) in leukocytes and DCs[8] survival (PI3K/Akt pathway)[9], and cytoarchitecture (Rho pathway) by regulating actin dynamics and endocytosis[10].

The initial step in the most basic model of chemokine-induced cell activation would be the binding of a monomeric chemokine to its corresponding monomeric GPCR, in our case we are

specifically interested in the CCR7 receptor and CCL19 interaction. Following receptor activation, as previously stated, the G protein α- and βγ-subunits separate to activate 'downstream' pathways, where the βγ-complex plays a crucial role in controlling cell migration.

The activation of G proteins is important for second messenger molecules like inositol phosphates and $Ca^{2+}$to activate a cascade of downstream molecules, such as protein kinase C as well as protein kinase B (PKB/Akt). Both kinases phosphorylate serine and threonine amino acid residues (Figure 1.1.2)[1]. PKC induces the activation of different signal transduction cascades. Therefore, the consensus is that binding of CCL19 to CCR7 receptor can catalyze distinct signaling pathways, The previous mentioned mechanism of activation of the GPCR by G protein described is one of three mechanisms of regulation of GPCR mediated signaling. There are two other mechanisms that can control the signaling cascades of GPCRs. Receptor desensitization by β-arrestin and receptor recycling[11].

Therefore, the binding of chemokines will decrease the surface-exposed receptors due to receptor internalization. This process is considered a regulatory mechanism, as it will influence and inhibit cellular responses and chemokine activity. GPCRs can be phosphorylated by specific kinases, G protein-coupled receptor kinases (GPCRKs or GRKs). Once the GPCR is phosphorylated it will become a docking site and recruit β-arrestin. Hence, both GRKs in tandem with β-arrestin will regulate the GPCR causing what we know as receptor desensitization because as the name suggests, when β-arrestin binds to GPCR it arrests its activity by inhibiting its ability to bind to the trimeric G protein. The last form of regulation of GPCR mediated signaling is by receptor recycling or internalization. β-arrestin can also act as an adaptor protein anchoring AP2- and clathrin to the receptor. The ability of β-arrestin to act as a scaffold protein will promote the signaling of the ERK pathway activation.

Several GPCRs undergo internalization through clathrin coated vesicles through which they are then recycled to the plasma membrane. It is then proposed that β-arrestin serve as clathrin adaptors in GPCR endocytosis. The clathrin coated pits will cause membrane invagination. Once inside the cytoplasm the receptor travels to endosomes that have a low hydrogen ion concentration, or a low pH. The receptor will then dissociate from the ligands becoming dephosphorylated and it is then that it is recycled back to the cell membrane or be further degraded by lysosomes[12].

The typical agonistic properties of CCL19 result in strong agonist-induced G protein activation, CCR7 phosphorylation, β-arrestin recruitment, desensitization of CCR7, and MAP kinase activation that is dependent on β-arrestin. The same amount of G protein activity results from the activation of CCR7 by CCL21, but there is significantly less overall phosphorylation and recruitment of β-arrestin. In cell lines and primary T cells, CCL19-mediated β-arrestin recruitment triggers receptor internalization, but CCL21 barely does. CCL21 is still able to stimulate β-arrestin-mediated ERK1/2 phosphorylation in CCR7 even when it only partially induces internalization. The conventional idea of GRKs as redundant kinases is likely oversimplified given the complexity of β-arrestin function. The expression of GRKs 2, 3, 5, and 6 is widespread. The degree to which they provide functional specialization versus redundancy is largely unknown, but there is recent evidence for the latter in some receptor systems. For example, it appears that only GRK5/6 is necessary for β-arrestin-mediated MAP kinase signaling. While GRK6 is unaffectedly activated by both CCR7 ligands, GRK3 activity is specific to CCL19, hence CCL19 stimulation results in more robust serine/threonine phosphorylation and greater β-arrestin recruitment.

Ca^{2+}-dynamics in the cytosol can be heavily influenced by the activation of GPCRs through their cascade signals. This is important because the dysregulation of Ca^{2+} can be modulated by GPCRs which is associated with the treatment of pro-inflammatory diseases. As it is well

understood Ca^{2+} serve as signal messenger inside the cell. These signals regulate various intracellular processes and speed up their signals at the specific time, meaning time dependent. Ca^{2+} can mediate intracellular responses by sensing effectors that translate Ca^{2+} signals into different spatiotemporal dynamics. Therefore, cells can reduce or spike their Ca^{2+} concentrations through GPCRs regulation. For instance, in the $G_{\alpha i/o}$, pathway the $G_{\alpha i/o}$ subunit of the G-protein can inhibit the cAMP production and voltage-gated Ca^{2+}[13].

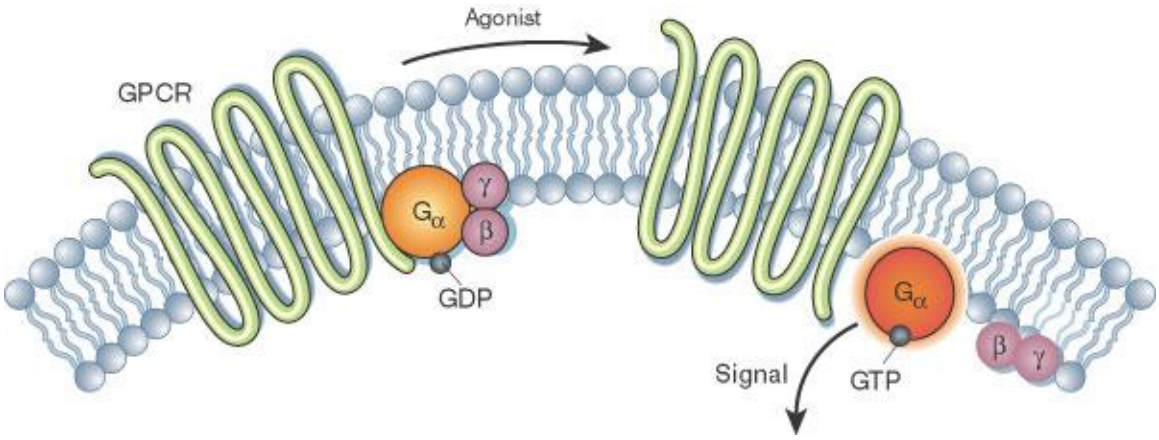

Figure 1.1.1 Activation of the G alpha subunit of a G-protein-coupled receptor
G alpha's (orange circles) interaction with GDP, G beta-gamma (purple circles), and a G-protein-coupled receptor in resting cells determines the state of the protein (GPCR; light green loops). The state of the receptor is altered when a ligand known as an agonist stimulates it. To activate G alpha, GTP must be exchanged for the bound GDP after G alpha separates from the receptor and G beta-gamma. The next step for G alpha is to activate further cell molecules[1].

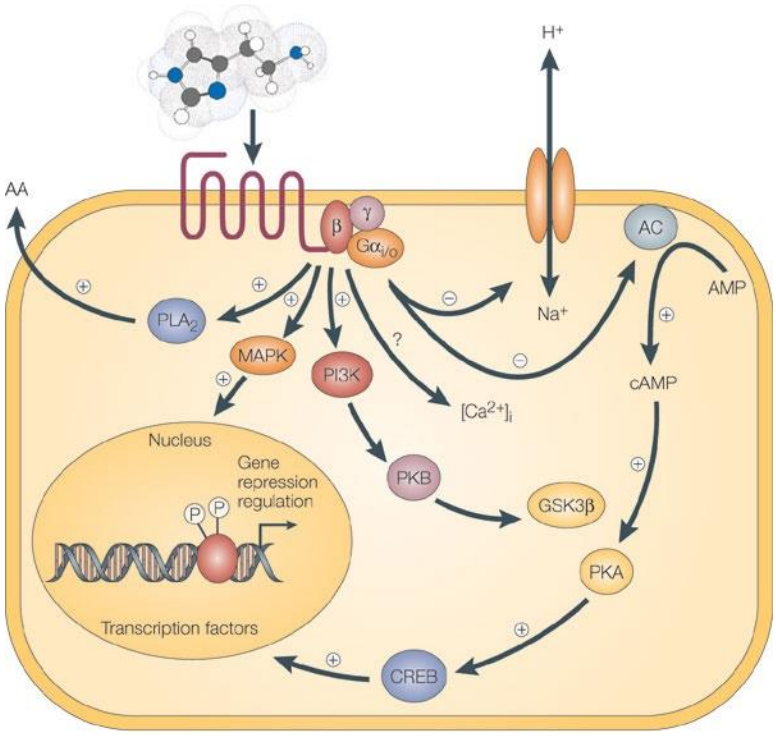

Figure 1.1.2 Signaling cascades within a cell.
An agonist triggers a cascade including G proteins and cAMP-related pathways that modulates cellular signaling when it binds to the plasma membrane's seven-transmembrane G-protein-coupled receptor[1].

Regarding chemokine receptor signaling in leukocytes, data supports that Gαi2 subunits are solely responsible for chemotaxis[14]. Chemokine receptor stimulation rapidly activates phosphoinositide-specific phospholipase C2 (PLC-2) and PLC-3 isoenzymes, resulting in the formation of inositol-1,4,5-triphosphate (InsP3) and a transient increase in the concentration of intracellular free calcium ($[Ca^{2+}]i$)[15]. Direct contact with βγ subunits that are released from the Gαβγ receptor complex activates the two PLC isoforms that are involved in chemokine-signal transduction[16,17]. The significance of $[Ca^{2+}]i$ increases in chemotaxis was further highlighted by the gene-targeting investigations. To enable appropriate and reversible contact of adhesion molecules with the substrate during chemotaxis, calcium is necessary in the extracellular media[18]. In addition to causing the creation of InsP3, chemokine-mediated activation of PLC also causes

the generation of diacylglycerol (DAG), which then triggers the activation of protein kinase C (PKC). The type IB phosphatidylinositol 3 kinase γ (PI3Kγ) is another recognized effector of subunits βγ[19]. Chemokines drive the quick synthesis of phosphatidylinositol 3,4,5-trisphosphate PtdIns(3,4,5)P_3 by this enzyme, which is then dephosphorylated to create PtdIns(3,4)P_2[20]. PKB is quickly activated and drawn to the membrane of the cell's forefront during G protein-coupled receptor-stimulated chemotaxis. The translocation of PHAKT-GFP25 and activation of PKB caused by chemoattractant are prevented by wortmannin or LY294002's inhibition of PI3Ks[21,22].

CCL19 and CCL21 share a conserved tetra-cysteine motif but only a 32% amino acid identity. CCL21 differs structurally from CCL19 uniquely by having a long C-terminal tail containing an extra 37 amino acids (6 cysteine residues). These amino acids are highly positively charged and capable of binding glycosaminoglycans (GAGs)[23]. Studies completed in modifying the C-terminus of CCL21 by removal of the differing 37 amino acids (tail-less CCL21) have shown the importance of the C-terminus tail (Figure 1.1.4)[3,24–26]. Modifications to either tail of CCL19 or CCL21 impacts the signaling pathway. CCL19 is secreted by mature dendritic cells (mDCs), whereas CCL21 is secreted from the endothelium of afferent lymphatic vessels. This has been shown in mice; however, there is a lack of evidence in humans. Both are predominantly secreted by the lumen of high endothelial venules, the stromal cells of the draining lymph node, and the spleen[27]. Because of their differing structures and expression patterns, CCL19 and CCL21 have different binding affinities for heparin or heparan sulfate. Therefore, the specificity of the binding sites of these chemokines triggers different second messengers and downstream adaptor components which activate different signaling cascades, signaling pathways, which are needed for *in vivo* functions or activities regarding immune responses [28].

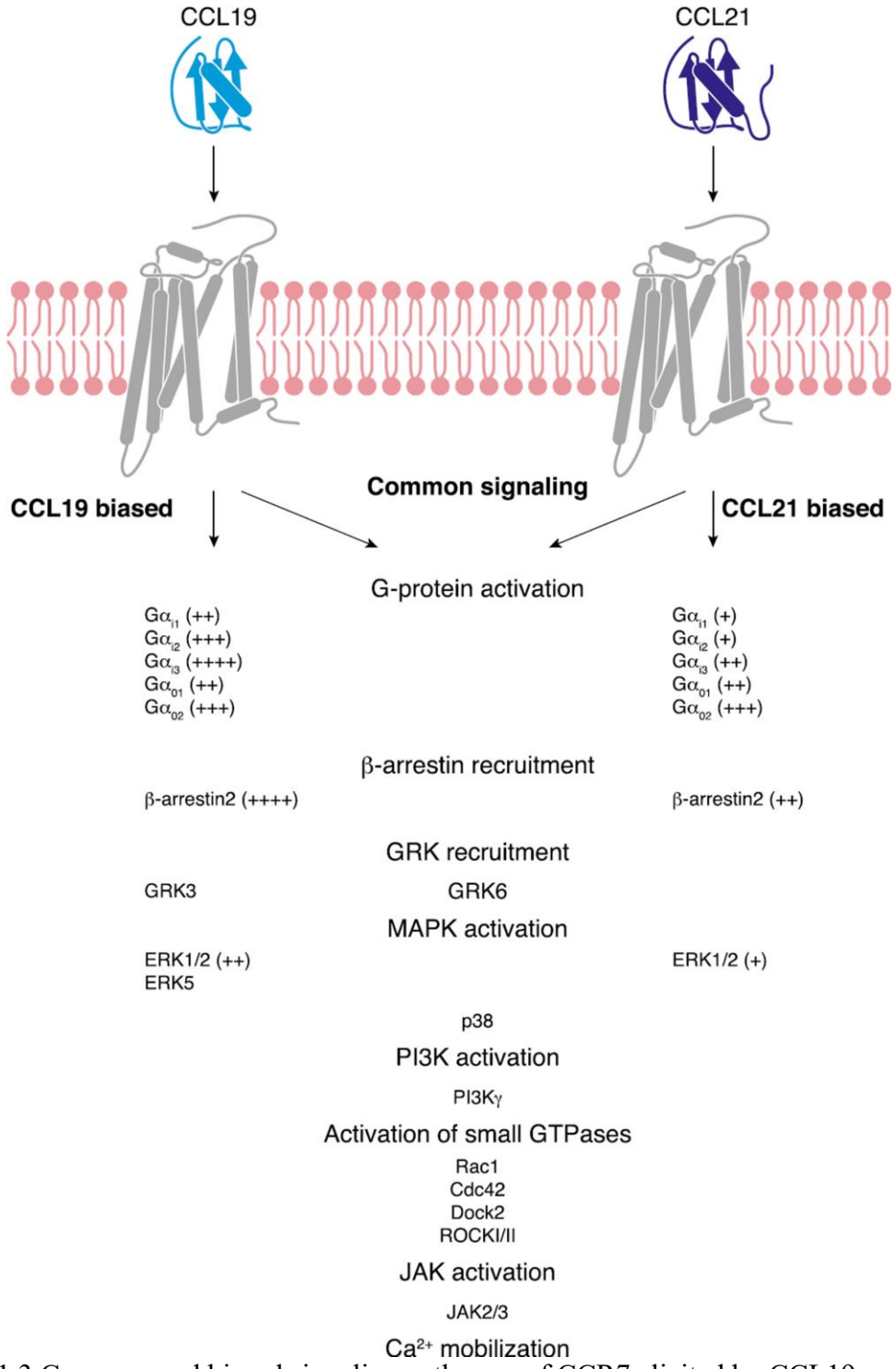

Figure 1.1.3 Common and biased signaling pathways of CCR7 elicited by CCL19 and CCL21. The G-protein coupling and activation that are induced by both CCR7 ligands have varying signal intensities, as denoted by plus signs[3].

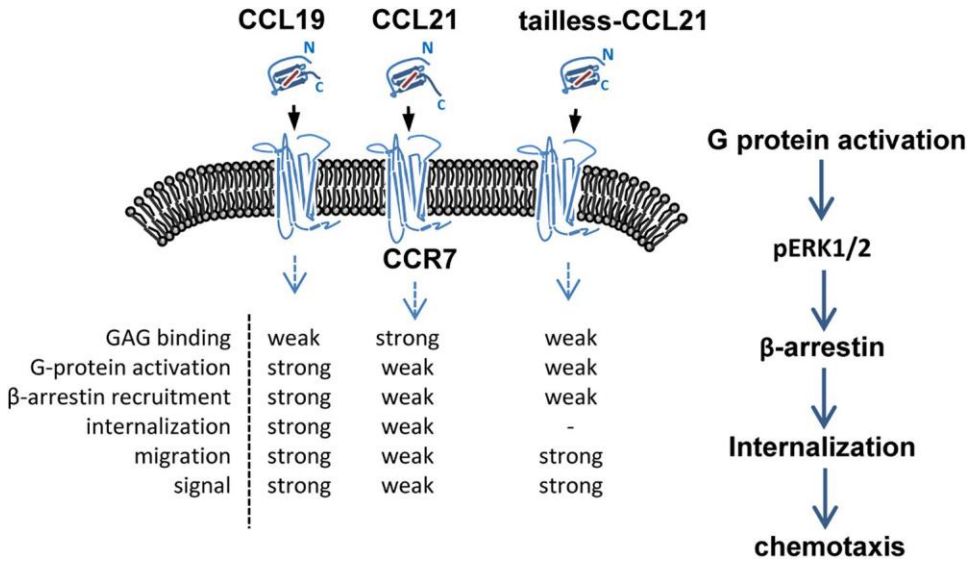

Figure 1.1.4 Overview of differences in signaling of CCL19, CCL21 and tailless-CCL21. Illustration using a schematic showing how CCL19, CCL21, and tailless-CCL21 affect various cellular responses.

The three following fundamental cellular responses are carried out by the CCR7-ligand axis: message acquisition, semantic extraction (or the identification of relations with respect of this receptor and ligands and their derived signaling pathways), and cell response induction. Chemokine receptor internalization is brought on by chemokine-receptor binding aids (or second messenger molecules) as well as RGS and GRKs that control chemokine activity by phosphorylation activating or deactivating the receptor consequently signaling pathways [29]. Only CCL19 has been found to efficiently promote CCR7 phosphorylation and internalization by β-arrestin. This results in receptor desensitization and antigen-presenting dendritic cell (DC) migration[30]. In contrast to CCL21, CCL19 clearly exhibits concentration- and time-dependent internalization in CD4+ and CD8+ T cells[31] (CCL21/CCR7 is also internalized but typically to a lower extent than CCL19/CCR7). Both ligands can induce Ca2+ mobilization, 3D chemotaxis, and activation of G-protein signaling; however, CCL19 has been found to be slightly more effective[30,31]. The binding of CCR7 to CCL19 can regulate T-cell activation, tolerance, and

inflammation as well as inflammatory responses[32]. CCR7 signaling also contributes to T cell development in the thymus and to lymphangenesis[33].

The improper regulation of these proteins can contribute to pathobiology of chronic inflammation, tumorigenesis, and metastasis, as well as autoimmune diseases[10,34,35]. Hence, chemokine signaling is an extensive study area for pharmaceutical intervention[36].

Antagonizing CCR7

A novel N-terminal truncation mutant of CCL19 (named $CCL19_{(8-83)}$) is a CCR7 antagonist that plays a role in a primary allogeneic immune response[37]. This antagonist specifically inhibits wild type CCL19 induced chemotaxis and intracellular calcium mobilization (Figure 1.1.5). This antagonist was first recognized in a characterization study of novel mCCL19 truncation mutants. The inclusion of additional amino acids before the conserved double cysteine in the sequence greatly impacts antagonistic properties. Treatment of mice with $CCL19_{(8-83);}$ however, did not globally inhibit the recruitment of cells into lymph nodes. Although, it does inhibit the generation of cytotoxic T lymphocytes toward allogeneic dendritic cells. The production of this antagonist was synthesized using tertiary N~-butyloxycarbonyl amino acid chemistry on an automated peptide synthesizer. This technique is expensive in upscaled productions and prone to errors in the synthesis of peptides.

The production of functional chemokines can be inherently challenging since chemokines must be folded properly to be functional[38]. Chemokines produced either by chemical synthesis or heterologous expression in *E. coli* are initially unfolded, unoxidized, and/or nonfunctional[39]. To produce functional proteins, synthetic or recombinant chemokines must be refolded, a process that requires cysteine oxidation to achieve the correct pattern of conserved disulfide bonds[40]. Many

researchers have adopted the protein SUMO (SMT3) as a fusion protein for chemokine production to take advantage of the SUMO-specific protease ULP1. ULP1 recognizes the SMT3 fold and cleaves the amide linking the SMT3 to the C-terminus of the chemokine. This system allows for the production of chemokines with native or altered N-termini[41,42].

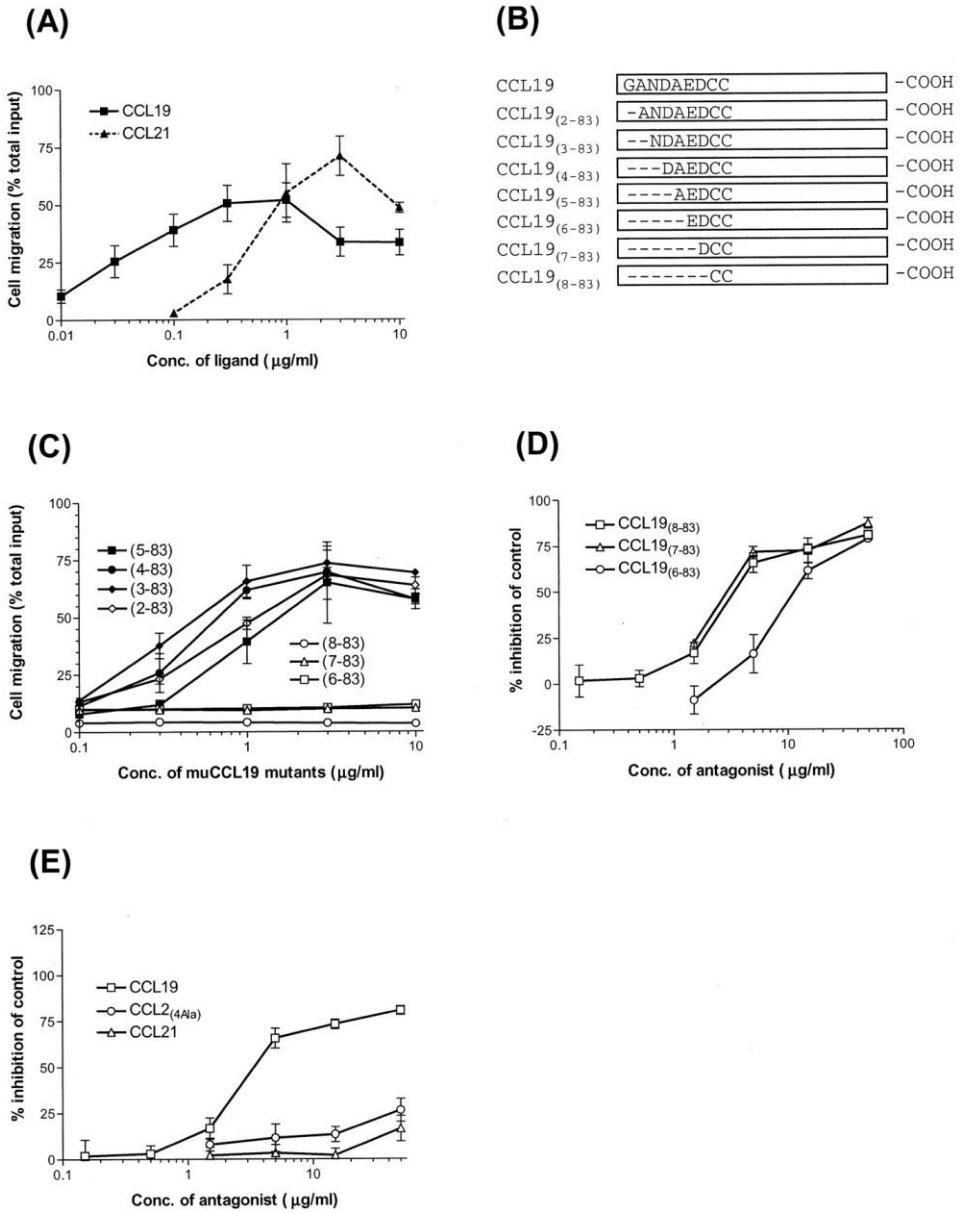

Figure 1.1.5 Development and characterization of mCCL19 truncation mutants.
The following results are from Pilkington (2004). Following 24 h of culture, cells were stained with 2 μm Calcein-AM and subjected to Transwell chemotaxis assays using mCCL19, mCCL21, or chemotaxis buffer alone. Values are the mean ± S.E. (CCL19, n = 12; CCL21, n = 8). B, the

CCL19 mutants used in this study. C, the ability of CCL19 mutants to stimulate chemotaxis of primary mouse splenocytes (n = 2 for $CCL19_{(6–83)}$ and $CCL19_{(7–83)}$; n = 4 for $CCL19_{(8–83)}$). D, the ability of $CCL19_{(6–83)}$, $CCL19_{(7–83)}$, and $CCL19_{(8–83)}$ antagonize wild type CCL19-induced chemotaxis (n = 2 for $CCL19_{(6-83)}$ and $CCL19_{(7–83)}$; n = 14 for $CCL19_{(8–83)}$. E, lack of antagonism of $CCL19_{(8–83)}$ toward wild type CCL21 (n = 4)[37].

T-cell acute lymphoblastic leukemia

Antagonizing CCR7 could be used as a potential target in clinical studies assisting in the treatment of T-cell acute lymphoblastic leukemia (T-ALL). T-ALL is an aggressive hematologic tumor resulting from the malignant transformation of T cell progenitors. The chemokine receptor CCR7 is the crucial adhesion signal necessary for the targeting of leukemic T cells into the CNS; this being suggested by T-ALL gene-expression profiling[43–45.].

Gene expression profiling of T-ALL with CNS involvement has identified a higher expression of CCR7 in those T-cells generating the basis for mouse studies. In a T-ALL mouse study, the silencing of CCR7 prevented the leukemic T-cells from infiltrating the CNS, clearly showing the importance of CCR7 in CNS infiltration of T-ALL [43–45.].

Human tumors with Notch1-activating mutations express the Ccr7 gene, which is regulated by the T-ALL oncogene Notch1 activity. At least 80% of T-ALL cases are thought to involve activation of the Notch1 signaling pathway. T-ALL accounts for 10%–15% of pediatric and 25% of adult ALL cases and is found more frequently in males than females[46,47]. Clinically, T-ALL patients show diffuse infiltration of the bone marrow by immature T cell lymphoblasts, high white blood cell counts, mediastinal masses with pleural effusions, and frequent infiltration of the central nervous system (CNS) at diagnosis[44,48]. The current treatment of T-ALL focuses on management of the disease. This is achieved by simultaneously employing both T- and B-cell acute lymphoblastic leukemia (ALL) regimens, incorporating induction, consolidation, delayed intensification, and maintenance with CNS prophylaxis consisting of high-dose and intrathecal

chemotherapy[49]. The percentage of patients that present with CNS involvement during adult T-cell lymphoblastic leukemia (T-LBL) and T-ALL varies but may be as high as 10%[50,51]. In addition, a high rate of CNS relapse was observed in earlier studies without specific CNS-directed prophylaxis[52]. The intensity of CNS-targeted therapy may be reduced by targeted suppression of CNS involvement in T-ALL, which would lessen the short- and long-term effects. Using the antagonist $CCL19_{(8-83)}$ we can attempt to reduce CNS involvement of T-ALL by antagonizing CCR7.

1.2 SPECIFIC AIMS

Perform in *vitro* assays to analyze the antagonistic properties of $CCL19_{(8-83)}$ in T-ALL by measuring inhibition of chemotaxis, calcium mobilization, and receptor internalization[53]. These are standard assays for verifying biological activity of chemokines prior to structural or functional research studies. We use a human derived T lymphoblast diseased with Acute Lymphoblastic Leukemia cancer model named CCRF-CEM as a pediatric T-ALL cell model to determine the molecular mechanisms for CCR7 activation. This will be combined with chemotactic assays *in vitro* to determine the molecular mechanisms driving T-ALL migration in response to CCR7 ligands. Second, the synthesis of $CCL19_{(8-83)}$ in *E. coli* using SUMO as a fusion protein for production of a functional antagonist. We hypothesized that $CCL19_{(8-83)}$ can inhibit the activation of the CCR7 receptor of these leukemic T cells therefore directly affecting chemotaxis.

To test this hypothesis, we performed the following specific aims:

Specific Aim 1: Assess $CCL19_{(8-83)}$ in biological activity assays *in vitro.* Chemotaxis assays were used to measure chemokine induced directional migration of cells across a semipermeable membrane toward CCL19. Migration to chemokines, is termed "chemotaxis". Our goal is to confirm that antagonist $CCL19_{8-83}$ inhibits chemotaxis. Calcium mobilization assays were used to determine if $CCL19_{8-83}$ inhibits the mobilization of cytosolic calcium (Ca^{2+}) ions that are released from the endoplasmic reticulum, as a result of CCR7/CCL19 activation in T cells. In these studies, we used T-ALL cancer cell lines CEM and HuT78. Internalization of CCR7 following binding to CCL19 can be analyzed by flow cytometry[54]. In the presence of $CCL19_{8-83}$, internalization of the receptor should be blocked in the presence of CCL19.

Specific Aim 2: Produce and purify antagonist $CCL19_{(8-83)}$ using a pSUMO-tag in *E. coli*. This method provides a source of biologically active proteins for *in vitro* or *in vivo* functional assay that is consistent with Current Good Manufacturing Practices (cGMP). For this process *E. coli* BL21(DE3) cells were transformed with plasmid pSUMO fused to $CCL19_{(8-83)}$ cDNA to produce 6His-SMT3-$CCL19_{(8-83)}$. For the removal of 6His-SMT3, ULP1 will be used. This will generate $CCL19_{(8-83)}$ with native N-terminus. The antagonist will be further purified using reverse phase HPLC and confirmed by tandem mass spectrometry.

Chapter 2: Assessment of Inhibition of Recombinant CCL19$_{(8-83)}$

2.1 Aim 1: Assessment of Inhibition of Antagonist In-Vitro

2.1.1 Rationale

There are a variety of methods for confirming chemokine biological activity, which were a necessary step before using recombinant chemokines in structural or functional research. Calcium mobilization, receptor internalization, and chemotaxis assays were used to test biological activity *in vitro*. Calcium mobilization assays measure the amount of the secondary messenger Ca^{2+} released in the cytosol as a result of chemokine receptor activation[55]. Chemotaxis experiments measure chemokine-directed migration of cells that express chemokine receptors through pores in a membrane separating the cells from the chemokine[56]. Clathrin-coated pits are used by several GPCRs to undergo agonist-induced endocytosis. Although this highly conserved method can endocytose GPCRs, they can still travel along separate downstream membrane pathways that perform various physiological tasks. After endocytosis, most β2-adrenergic receptor (β2AR) are recycled back to the plasma membrane within 30 minutes. Rapid recycling of the β2AR is well established to play an important role in signal transduction functional resensitization. We routinely employ fluorescence activated cell sorting (FACS) based flow cytometry as a quantifiable tool for assessing receptor internalization and recycling. In the most basic application, a fluorescent antibody conjugate is used to detect receptors on the cell surface before, during, and after agonist exposure, and then again after agonist removal. Changes in surface receptor levels are then tracked over time. This enables the use of kinetic models to estimate receptor internalization and recycling rates[57].

For these assays, assessment of the inhibitor was completed by purchasing it from a biotechnology company based in China. Many potential biotechnology companies offering peptide

synthesizing services located within the United States did not accept or provide services for proteins at the length of our antagonists. As previously mentioned, synthesizing a protein at the length of the antagonist, 76 AA long, is inherently difficult and prone to errors, directly influencing monetary cost.

2.1.2 Materials and Methods

Cell Lines

HuT-8 and CCRF-CEM cell lines were obtained from the American Type Culture Collection (ATCC) and cultured in complete RPMI 1640 (RPMI 1640 medium (Invitrogen), 10% heat-inactivated FBS (Gibco), and 2 mM L-glutamine (Invitrogen)) at 37°C in a humidified atmosphere of 5% CO_2. Roswell Park Memorial Institute (RPMI).

Chemotaxis Assay

A 48-well chemotaxis chamber was used for all chemotaxis assays (Neuro Probe). Using a 10 μm pore nitrocellulose membrane (Neuro Probe) that had been preincubated in 10 μg/ml fibronectin, the upper wells containing $5x10^6$ cells per mL were separated from the lower wells, which were loaded with 0 or 10 nM to 1 μM hCCL19 with serum-free (sf) RPMI 1640 medium (Sigma). Cells were allowed to migrate for 90 min. to hCCL19 gradients in a humidified, 37°C, 5% CO_2 chamber. After migration, chambers were taken apart, polycarbonate membranes were preserved in 100% methanol, and 4′,6-diamidino-2-phenylindole (DAPI) was used to stain them. All migration results were standardized to the migration of cells to sfRPMI 1640 media, which was used as the "0" migration point in each test.

Calcium Mobilization

Hanks' buffered saline solution with calcium and magnesium (HBSS) was used to resuspend the centrifuged cells at a concentration of $5x10^6$ cells per mL after they had been washed once in PBS. The cells were treated for 45 minutes with 4 μM Fluo4-AM/0.1% Pluronic F-127 at 37 °C, washed once with HBSS, and then further incubated for 45 minutes at 37 °C. Cell were washed once more with HBSS, then resuspended at $2x10^6$ cells per mL in HBSS. The cells were stimulated with hCCL19 and continuously measured for fluorescence using a Fluoroskan™ Microplate Fluorometer (Thermo Scientific) at Ex494/Em506.

Receptor Internalization Assays

Lymphocyte suspension cells were isolated from flasks, counted, and washed in PBS. 100 μL of sfRPMI 1640 with $5x10^6$ cells per ml were utilized for each time point. Cells were treated with 200 nM CCL19 for the indicated times after a 10-min preincubation at 37°C. The addition of 10 volumes of ice-cold sfRPMI 1640 stopped internalization. PE-conjugated anti-human CCR7 antibodies were used to label cell surface receptors for 30 minutes on ice, followed by three rinses with ice cold PBS. Cells were either immediately tested or fixed in 2% paraformaldehyde and kept at 4°C for up to four days. Using a Gallios (Beckman Coulter), flow cytometry was used to measure the receptor levels. Using [mean channel fluorescence of PE-anti-CCR7 at time-point]/ [mean channel fluorescence of PE-anti-CCR7 at time = 0], the mean percent of receptor remaining on the surface of cells was calculated.

Ligands

Synthetic antagonist $CCL19_{(8-83)}$ was purchased from PepMic (Gusu District, Suzhou, China) using their custom peptide synthesis services. Agonist hCCL19 was purchased from Shenandoah Biotechnologies (Santa Ana, California, United States).

2.1.3 Results

Chemotaxis Assay of CCRF-CEM Cells to CCL19 and Inhibition

To develop the assay for characterization of the antagonist, chemotactic dose response curves to hCCL19 was generated using the CCRF-CEM cell line. The expected bell-shaped curve was obtained in response to CCL19. CCL19 induced detectable migration at 20 nM and maximal chemotaxis at 60 nM (Figure 2.1.1). Optimal migration of ~50% of the total input cells (EC50) was identified at a concentration 32 nM for CCL19. This value was used for in-vitro chemotaxis inhibition assays to assess and characterize the $CCL19_{(8-83)}$ antagonist.

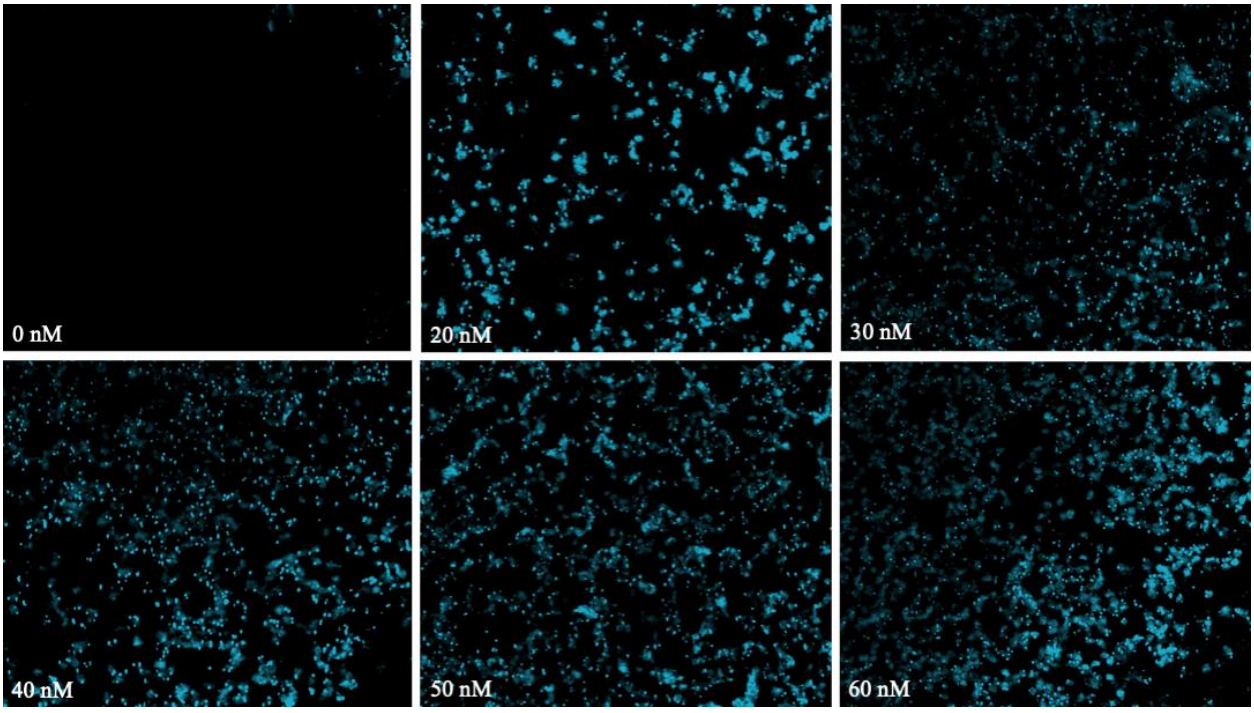

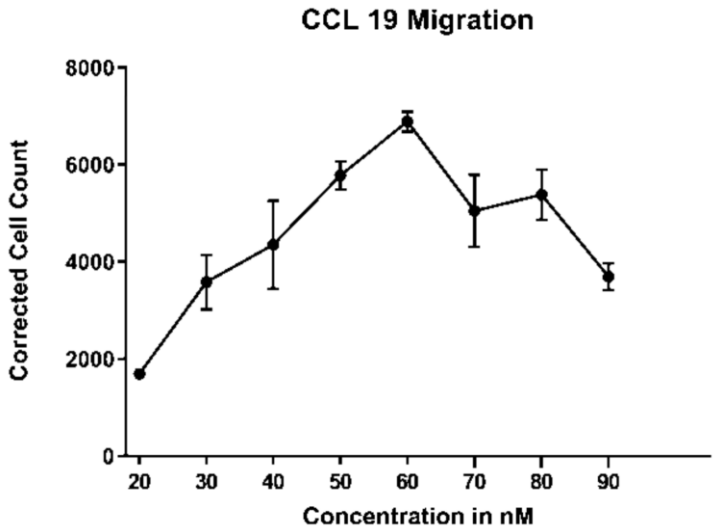

Figure 2.1.1 Chemotactic Dose Response to CCL19.
Transwell chemotaxis assay for CCRF-CEM, cells were counted by confocal microscopy in capture images. N=3 with error bars indicating standard deviation.

Next, to assess the antagonistic effects of $CCL19_{(8-83)}$ we used inhibition assays in the presence of a gradient of the antagonist. Cells were preincubated with the antagonist and then loaded to the Boyden top chamber, for induction of chemotaxis CCL19 at 32 nM was added in the bottom chambers. At concentrations as low as 18 nM of $CCL19_{(8-83)}$ we observe inhibition of wild type CCL19-mediated chemotaxis at a concentration of 32 nM (Figure 2.1.2). Chemotaxis was almost completely inhibited when the antagonist was used at a concentration of 1800 nM, the optimal inhibitory effect (IC50) was identified at 42 nM.

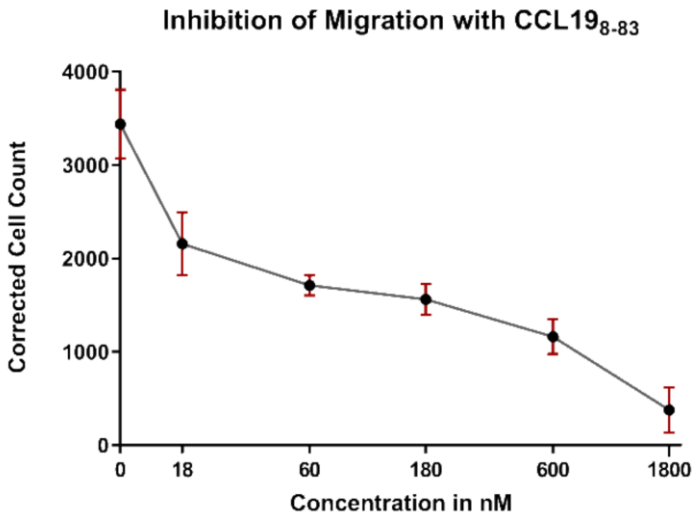

Figure 2.1.2 CCL19$_{8-83}$ antagonizes wild type CCL19-induced chemotaxis. Analysis of inhibition of chemotaxis in Boyden chamber assay with the use of antagonist. N=3, error bars indicate standard deviation.

Calcium Mobilization Assay of CCRF-CEM Cells to CCL19

Following determination of the EC50 for CCL19 in the chemotaxis assay a new dose response for calcium mobilization was completed to reassess CCR7-CCL19 activation of the activation pathway. Calcium mobilization assay was analyzed using the CCRF-CEM cell line the presence of a range of (25 – 200 nM) hCCL19 and assessed by binding of a fluorescent dye. The results obtained did not follow the previous results for the chemotaxis assay, instead a linear relationship between dose response was established. The bell-shaped dose response obtained in the chemotaxis assay was not observed. An increase in calcium mobilization continued as concentration of hCCL19 increased with a maximum Ca2+ signal at 200 nM hCCL19 (Figure 2.1.3).

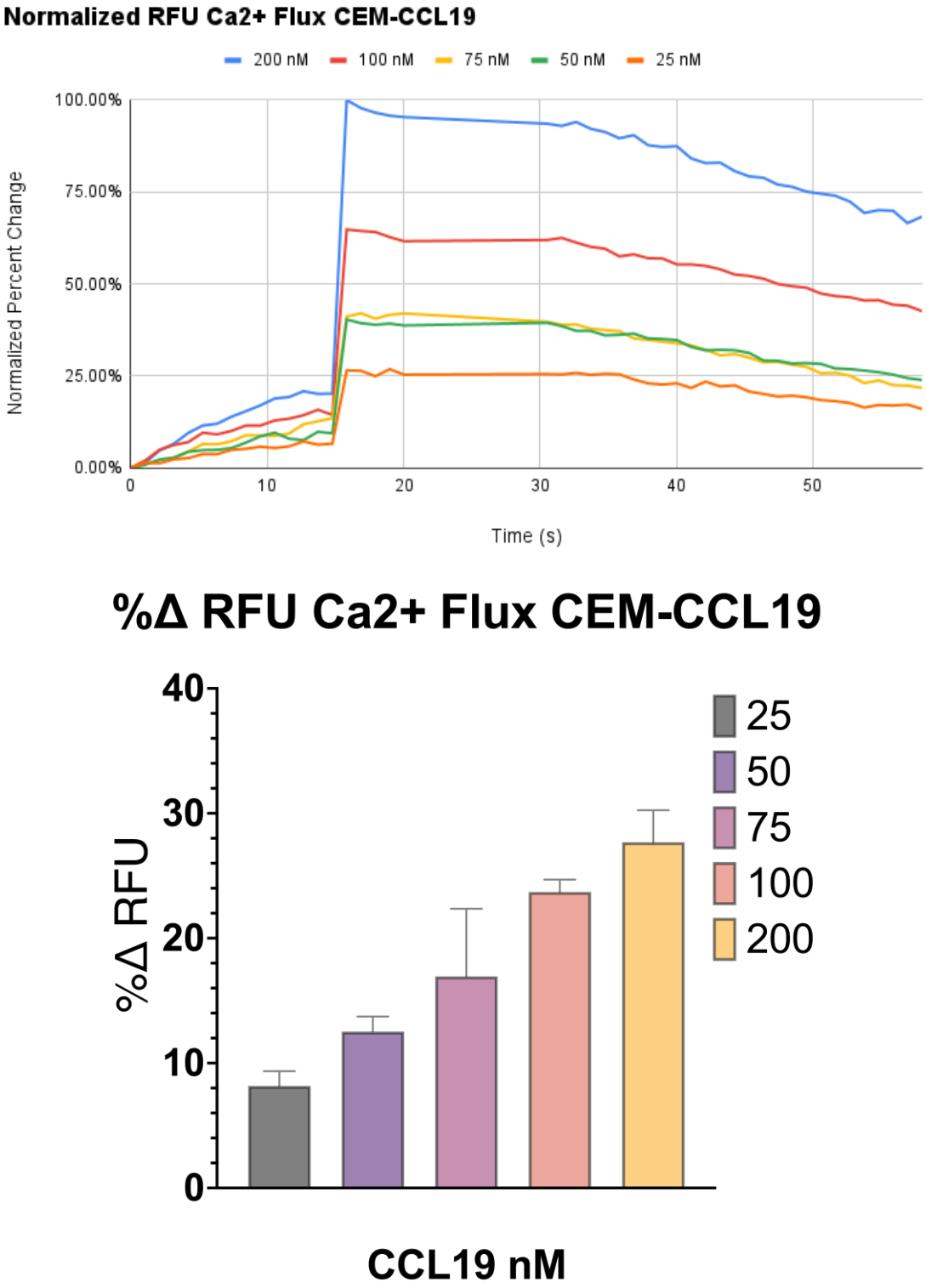

Figure 2.1.3 Calcium Flux Response to CCL19

Completion of calcium mobilization assay indicates a linear dose response as a change from baseline as percent increase. N=3 with $p<0.0001$ for group-wise comparison analysis.

Receptor Internalization Assay of CCR7 to CCL19

Analysis of receptor internalization using CCRF-CEM cells with stimulation of CCR7 using 32 nM hCCL19 at two time points showed a decrease in as measured by flow cytometry (Figure 2.1.4). The level of CCR7 on the cell surface decreased ~25% at both 30s and 60s exposure stimulation with hCCL19. Cells treated with 43 nM of the antagonists did not show a decrease in CCR7 on the cell surface once stimulated with 32 nM of hCCL19, indicating the receptor was not internalized after stimulation due to inhibition.

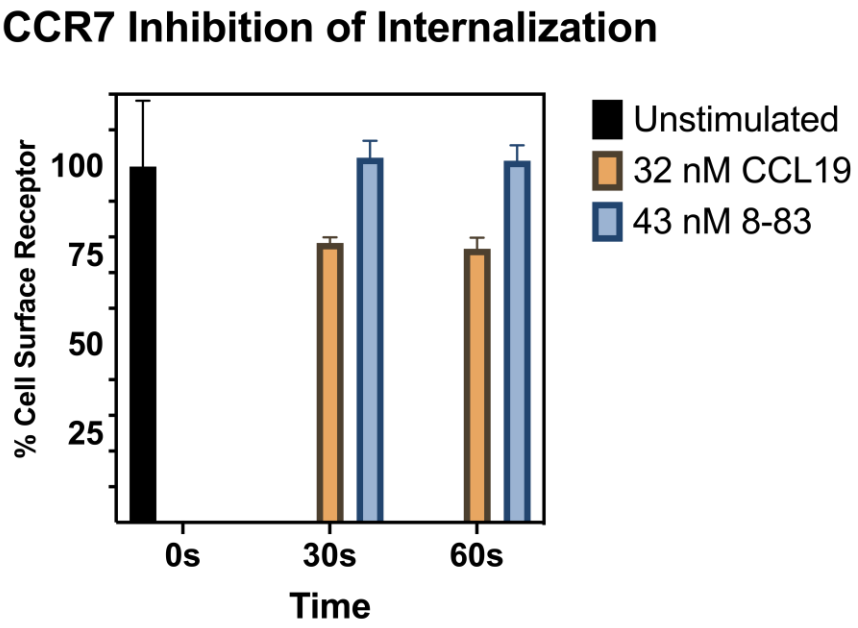

Figure 2.1.4 CCRF-CEM CCR7-CCL19 Receptor Internalization
Data obtained from flow cytometry using anti-hCCR7 fluorescent antibody, error bars indicate mean value.

2.1.4 Discussion

Using the antagonist $CCL19_{(8\text{-}83)}$ showed a decrease in CCR7-CCL19 directed chemotaxis at a low concentration. Chemotaxis experiments indicate a dose-response to CCL19 in a bell-shaped response, the antagonists have a linear dose response to inhibition of chemotaxis. The concentration to direct chemotaxis in CCRF-CEM cells in CCR7 to CCL19 exhibited an EC50 at

32 nM of hCCL19, the antagonist $CCL19_{(8-83)}$ exhibited an IC50 at 42 nM in this assay. This small concentration of antagonists makes it highly effective with an immense potential for further use. The data obtained from calcium mobilization assays indicate the effective dose of CCL19 to illicit a response differs in the signaling pathway of analysis, calcium mobilization data did not have a bell-shaped dose response as did the chemotaxis assay. The potential maximum response from calcium mobilization data was not identified as the range tested for hCCL19 did not exceed 200 nM in any assay completed. It is possible with a greater dose range a better understanding of the calcium movement could be understood. Internalization data using the antagonists indicated at the tested concentration based on EC50 and IC50 from the chemotaxis assay showed the antagonists stopped receptor internalization.

Chapter 3: Development of Recombinant Antagonist

3.1 Aim 1: Development and Purification of Recombinant CCL19$_{(8-83)}$

3.1.1 Rationale

The generation and purification of recombinant proteins is an important technique in the advancement of biosciences, improvements in biotechnology have allowed for ease in acquiring bioactive proteins. Biologically active proteins are necessary for any functional assay creating a need for a reliable source and a demand for efficient methods. A bioactive chemokine protein supply is critical to the study of chemokine function and to be fully active the protein must be correctly folded. The production of functional chemokines can be intrinsically difficult due to chemokine folding[38,58]. For instance, chemokines, whether produced by chemical synthesis or by heterologous expression in *E. coli*, are first unfolded, not oxidized and non-functional. Synthetic or recombinant chemokines must be folded to become functional, a process that necessitates cysteine oxidation to generate the correct pattern of disulfide linkages[59–62]. Another challenge with creating functional recombinant chemokines is that they are secreted proteins *in vivo*, and the mature N-terminus that emerges from removing the chemokine signal sequence is required for activity. As a result, removal of any fusion proteins or purification tags used in the making recombinant chemokines must leave only a native, mature N-terminus.

The invention of regulatable promoters, co-expression with chaperones and foldases, and the use of protein fusions are a few of the technological advances that have advanced recombinant protein expression in *E. coli*. Protein fusions have improved recombinant protein expression and solubility. Fusion systems boost protein expression, minimize recombinant protein proteolytic degradation, improve protein folding and solubility, and facilitate purification and detection. Maltose-binding protein (MBP), glutathione S-transferase (GST), thioredoxin (TRX), NUS A,

ubiquitin (UB), and SUMO are some of the fusion motifs. In eukaryotes, SUMO (small ubiquitin-related modifier), a 100-residue protein, affects protein structure and function by covalently modifying target proteins. In yeast, there is only one SUMO gene (SMT3), but vertebrates have three (SUMO-1, SUMO-2, and SUMO-3). SMT3 can be readily cleaved by ubiquitin like protease-1 (ULP1 or SUMO-protease-1) with fidelity and efficiency[63]. This system allows for the synthesis of chemokines with native or modified N-termini because ULP1 binds the SMT3 fold and cleaves the amide bond at the SMT3 C-terminus[64]. Using ULP1 to remove the His6-SMT3 from the chemokine produces a native, mature chemokine N-terminus.

3.1.2 Materials and Methods

Expression Plasmid

Synthetic cDNA encoding murine $CCL19_{(8\text{-}83)}$ plasmids were constructed by DNA2.0 by optimizing for codon usage in *E. coli.* strains DH5α and TOP10 (Invitrogen) were used for plasmid construction and manipulation, and pSUMO (A generous gift from Dr. Todd Holyoak, University of Waterloo) was used as the backbone. The cloning strategy used XbaI and XhoI sites upstream and downstream, respectively, of the fusion tag sequence, which was ligated to pSUMO-T7Kan vector (Figure 3.1.1).

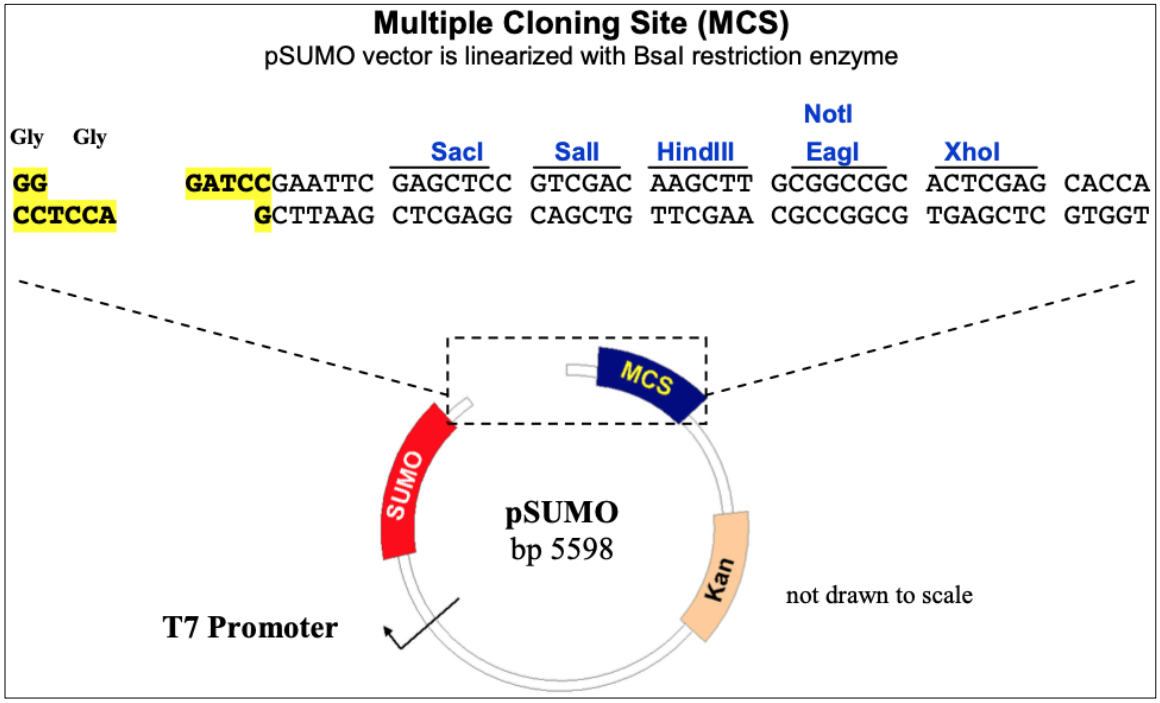

Figure 3.1.1 The pSUMO Plasmid.
MCS sites and sequence insertion point highlighted in yellow.

Protein Expression

Briefly, a single colony of pSUMO-CCL19$_{(8\text{-}83)}$ transformed BL21 (DE3) (Novagen) was inoculated into 10 mL of LB-broth with kanamycin (50 µg/mL) and grown overnight at 37°C with shaking (300rpm). Five milliliters of this overnight culture were inoculated into 1 L of Terrific-Broth (TB) (50 µg/mL Kan), and the culture was grown to OD_{600} = 0.6-0.8 at 37°C with shaking. Once an OD_{600} of ~0.7 was reached, expression was induced by adjusting the culture to 2 mM isopropyl-β-D-thiogalactopyranoside (IPTG) and incubating at 18°C with shaking. After 18 hours cells were harvested by centrifugation at 5,000 x g and stored at −80 °C.

Protein Purification

Cell pellets were resuspended in 10 mL of buffer A (50 mM sodium phosphate pH 8.0, 300 mM sodium chloride, 10 mM imidazole, 1 mM phenylmethylsulfonyl fluoride (PMSF), and 0.1%

(v/v) 2-mercaptoethanol). Cells were lysed by pulsed sonication at ~25% power for 10-seconds-on 10-seconds-off to prevent sample heating for 15 minutes. The lysed culture was centrifuged at 15,000 x *g* @ 4°C for 30 minutes, and the supernatant was isolated and stored at -80°C (soluble protein sample). The insoluble inclusion body pellet was solubilized using buffer AD (50 mM sodium phosphate pH 8.0, 300 mM NaCl, 10 mM imidazole, 6 M guanidine hydrochloride, and 0.1% (v/v) 2-mercaptoethanol) and clarified by centrifugation at 15,000 x *g* for 30 minutes. Supernatant containing the fusion protein, 6His-SMT3-CCL19$_{(8\text{-}83)}$ was loaded into a prepared 3 mL HisPur Ni-NTA Spin Column (Thermo Scientific) and incubated for 30 minutes in an end-over-end rotor at 4°C. The column was washed four times with 12 mL of Buffer AD and eluted with buffer BD (50 mM sodium acetate pH 4.5, 300 mM NaCl, 10 mM imidazole, and 6 M guanidine hydrochloride). The eluted 6His-SMT3-CCL19$_{(8\text{-}83)}$ was adjusted to 0.6% (v/v) trifluoroacetic acid and loaded into a prepared Discovery DSC-18 SPE Tube, 3 mL, (Supelco). The SPE tube was washed three times with 3 mL of buffer C (5% acetonitrile, 0.6% trifluoroacetic acid) and eluted with buffer CE (80% acetonitrile, 0.6% trifluoroacetic acid), the eluted sample was frozen and lyophilized. The lyophilized protein was refolded by infinite dilution into buffer R (50 mM bicine pH 8.5, 150 mM sodium chloride, 10 mM cysteine, 0.5 mM cystine, 1 mM ethylenediaminetetraacetic acid, 10% (v/v) glycerol) and incubated with stirring overnight at 4°C. Sample was diluted by twice the volume using Buffer RD (50 mM bicine pH→8.5, 1 mM ethylenediaminetetraacetic acid, 10% (v/v) glycerol) and added ULP1 enzyme (Sigma Aldrich), incubated with stirring overnight at 4°C. Digested protein sample was loaded into a prepared 1 mL HiTrap Q FF anion exchange chromatography column (Cytiva) and using the ÄKTA prime plus chromatography system (Cytiva) sample was eluted using a gradient from 0% buffer FA (50 mM bicine pH 9.0, 50 mM sodium chloride, 10 mM cysteine, 0.5 mM cystine, 2% (v/v) glycerol, and

0.02% (v/v) tween-20) to 100% buffer FB (50 mM bicine pH 9.0, 1 M sodium chloride, 10 mM cysteine, 0.5 mM cystine, 2% (v/v) glycerol, and 0.02% (v/v) tween-20) within 70 mL in 2 mL fractions. Fractions pooled together after SDS-PAGE analysis and further purified using SPE as pert previous methods.

Western Blot Analysis

Protein samples were prepared using Fluorescent Compatible Sample Buffer (Invitrogen) with 250 mM Dithiothreitol (DTT) and denatured by heating at 85°C for 5 minutes. Western blot analysis was performed using conventional protocols. The protein samples were separated by 10% Tricine protein gel, proteins were transferred to a low-fluorescence polyvinylidene difluoride (PVDF) membrane (Invitrogen). The blots were blocked with 4% bovine serum albumin (BSA cat#: 9998S, Cell Signaling Technology) in phosphate buffered saline (DPBS cat#: 17-512F, Lonza) containing 0.1 % Tween-20 (PBS-T) for 1 hour at 4°C. Membranes were immunoblotted with specific primary antibodies and incubated with corresponding fluorescent conjugated secondary antibody. The antibodies used in the western blot were as follows: Antibodies against CCL19 (0.25 μg/mL cat#: PA5-78936, Invitrogen), SUMO (1:1,000 cat#: 200-401-428S, Rockland Imunochemicals, and 6His (1:1,000 cat#: 1008288, Qiagen); secondary antibodies used for immunodetection were as follows: Alexa Fluor Plus 680 goat anti-rabbit IgG (0.1 μg/mL cat#: A32734, Invitrogen), Alexa Fluor 594 donkey anti-mouse IgG (1:5,000 cat#:715-585-151, Jackson ImmunoResearch), and Alexa Fluor Plus 555 goat anti-rabbit IgG (0.1 μg/mL cat#:A32732, Invitrogen). All immunoblots were visualized by fluorescence analysis in iBright FL1000 Imaging System (Invitrogen) and the optical density of each band was measured using the iBright Analysis Software.

MALDI-TOF MS Analysis

For MALDI-TOF MS (Matrix-Assisted Laser Desorption/Ionization Time-of-Flight Mass Spectrometer), analysis was completed using 80 µg of isolated protein sample. Sample was adjusted to 0.6% (v/v) trifluoroacetic acid and loaded into a prepared Pierce C-18 Tips (Thermo Scientific) for sample clean-up. The C-18 Tip was washed 3 X with 100 µL of buffer C (5% acetonitrile, 0.6% trifluoroacetic acid) and eluted with buffer CE (80% acetonitrile, 0.6% trifluoroacetic acid). The eluted sample was directly loaded into a Fleximass-DS polymeric MALDI MS sample plate. Analysis was performed on a MALDI-8020 MALDI-TOF mass spectrometer (Shimadzu Scientific Instruments, Columbia, MD).

3.1.3 Results

Construction of Recombinant 6His-SMT3-CCL19$_{(8-83)}$ Plasmid

Sequence for CCL19 was obtained by cDNA extraction from HuT78 (cat#: TIB-161, ATCC) reverse transcribed from mRNA to cDNA by PCR starting at cysteine C33 (Figure 3.1.2).

Figure 3.1.2 Amino Acid Sequence for CCL19$_{(8-83)}$.
The first conserved cysteine at position 33. The region highlighted in yellow is the original mCCL19 sequence, the conserved cysteine disulfide bonds are indicated in green.

DNA sample was cloned and sequenced. DNA sequence was optimized for codon expression in *E. coli* bacterium by (DNA2.0) and ligated into pSUMO. Plasmid construct was

transformed into *E. coli* DH5α and inoculated in LB media, plasmid was isolated from and sequenced for confirmation.

Recombinant 6His-SMT3-CCL19$_{(8-83)}$ Expression and Solubility

Plasmid construct was transformed into *E. coli* BL21(DE3), inoculated into TB media and induced with IPTG. Culture was collected and processed to analyze protein solubility by total cell lysis of the soluble fraction and insoluble fraction solubilized by using urea. Analysis by western blot for anti-CCL19 revealed protein is found in the insoluble fraction (Figure 3.1.3).

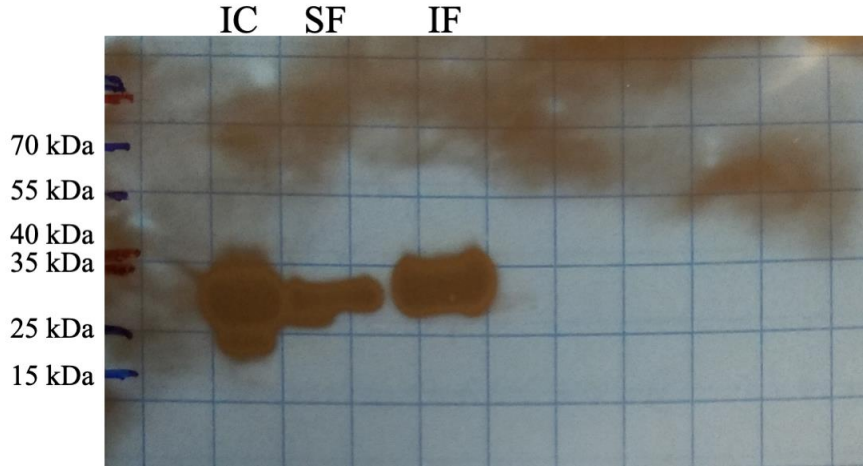

Figure 3.1.3 Western Blot Analysis of the Induced Transformed Bacterium. BL21(DE3) culture expressing 6His-SMT3-CCL19$_{8-83}$. Samples shown, induced culture (IC), soluble (SF), and insoluble fraction (IF).

Protein induction methods were tested for optimizing protein expression in TB media culture, testing concentration of IPTG, induction time and induction temperature. Results show protein expression at 18°C for 16 hours with 2 mM of IPTG to be the best induction method (data not shown).

Isolation of 6His-SMT3-CCL19$_{(8-83)}$ by Ni-NTA Spin Columns

A culture of transformed *E. coli* BL21(DE3) with plasmid construct was lysed by sonication and the soluble fraction was prepared for Ni-NTA spin column purification. Analysis of the samples collected from purification by SDS-PAGE shows a band below 25 kDa, matching the expected molecular weight (Figure 3.1.4). Samples were further analyzed by western blotting for anti-CCL19, data shows a correlating band at the expected molecular weight (Figure 3.1.5). Results from SDS gels also show some unknown contaminants, it is possible protein degradation has occurred by either sample heating during sonication or protein digestion by proteases.

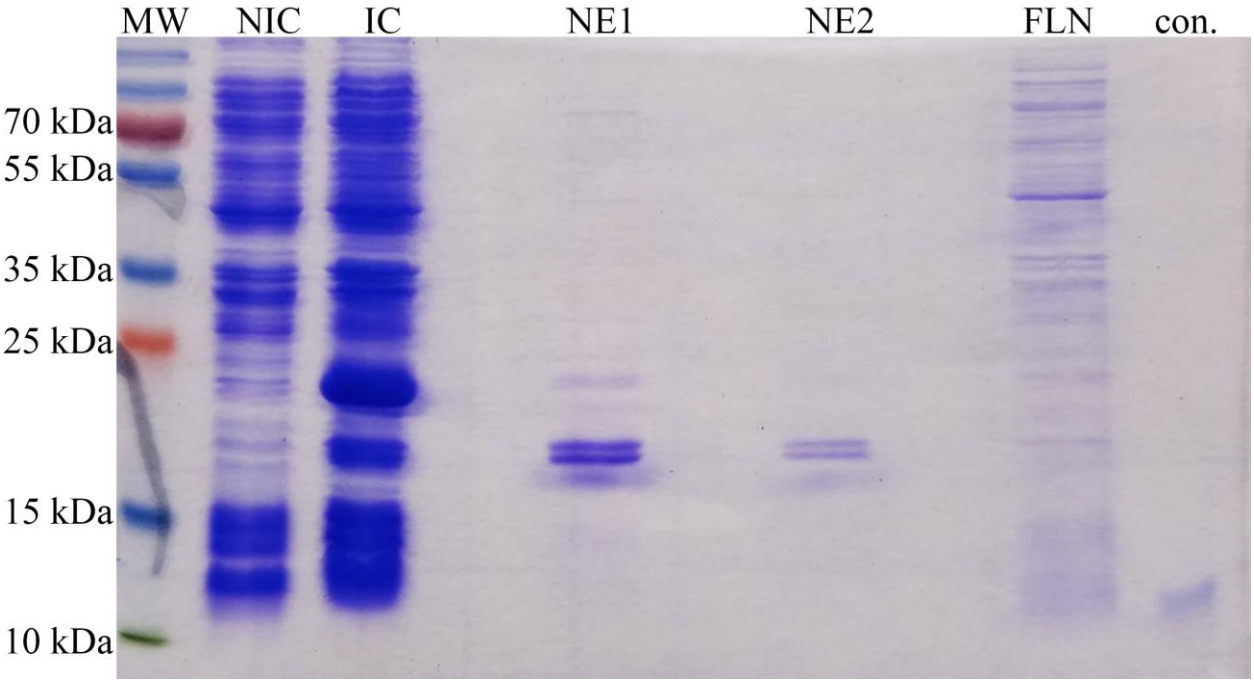

Figure 3.1.4 SDS-PAGE Analysis of Ni-NTA Spin Columns.
The induced culture (IC) exhibits a strong band above the 15 kDa marker not observed in the not-induced culture (NIC). native elution 1 (NE1) and native elution 2 (NE2). The remaining samples induced culture (IC), flow through native (FLN), and control hCCL19 (con.).

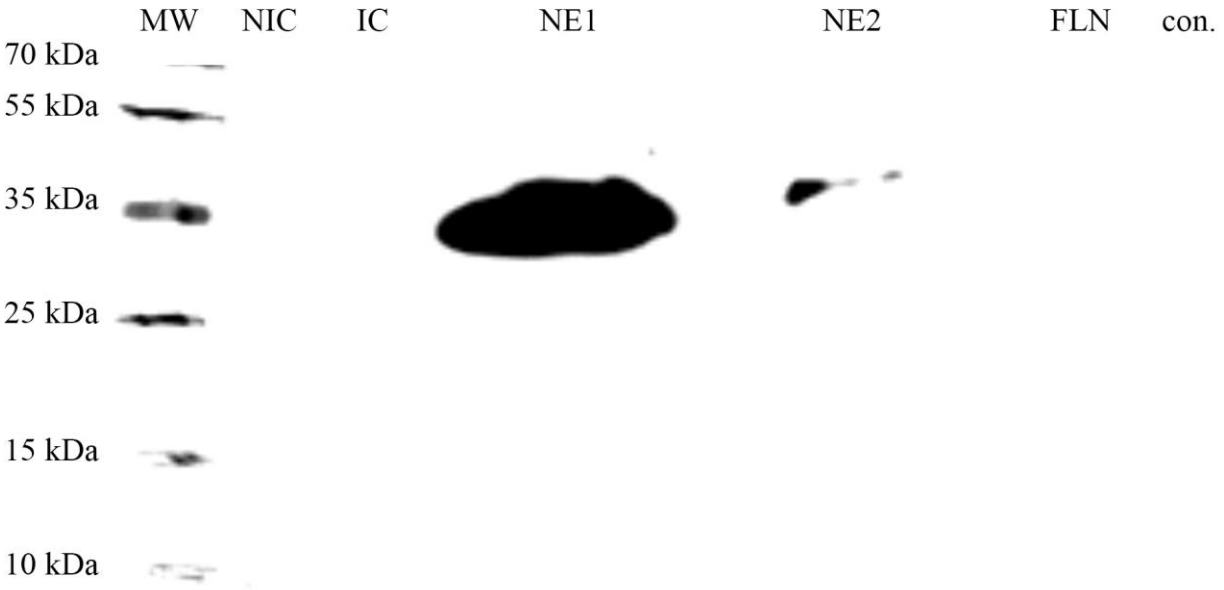

Figure 3.1.5 Western Blot of previous SDS gel from Ni-NTA Spin Columns.
Western blot analysis of samples for anti-CCL19 above the 25 kDa marker. Samples included, not induced culture (NIC), induced culture (IC), native elution 1 (NE1), native elution 2 (NE2), flow through native (FLN), and control hCCL19 (con.).

Digest of SMT3 by ULP1

Samples from Ni-NTA magnetic beads elution's were quantified using standard BCA quantification methods. Due to ULP1 recognition of tertiary structure of SMT3, elution samples need to be refolded. Elution samples were dialyzed in Tris buffer overnight using a 3,000 molecular weight cut-off (MWCO) dialyses unit. Dialyzed sample was added to the ULP1 enzyme and incubated overnight at 4°C. Analysis by SDS-PAGE revealed the protein sample was not digested, and sample loss had occurred during the process (Figure 3.1.6). Protein aggregation is thought to be the most likely explanation for loss of sample and failed digest.

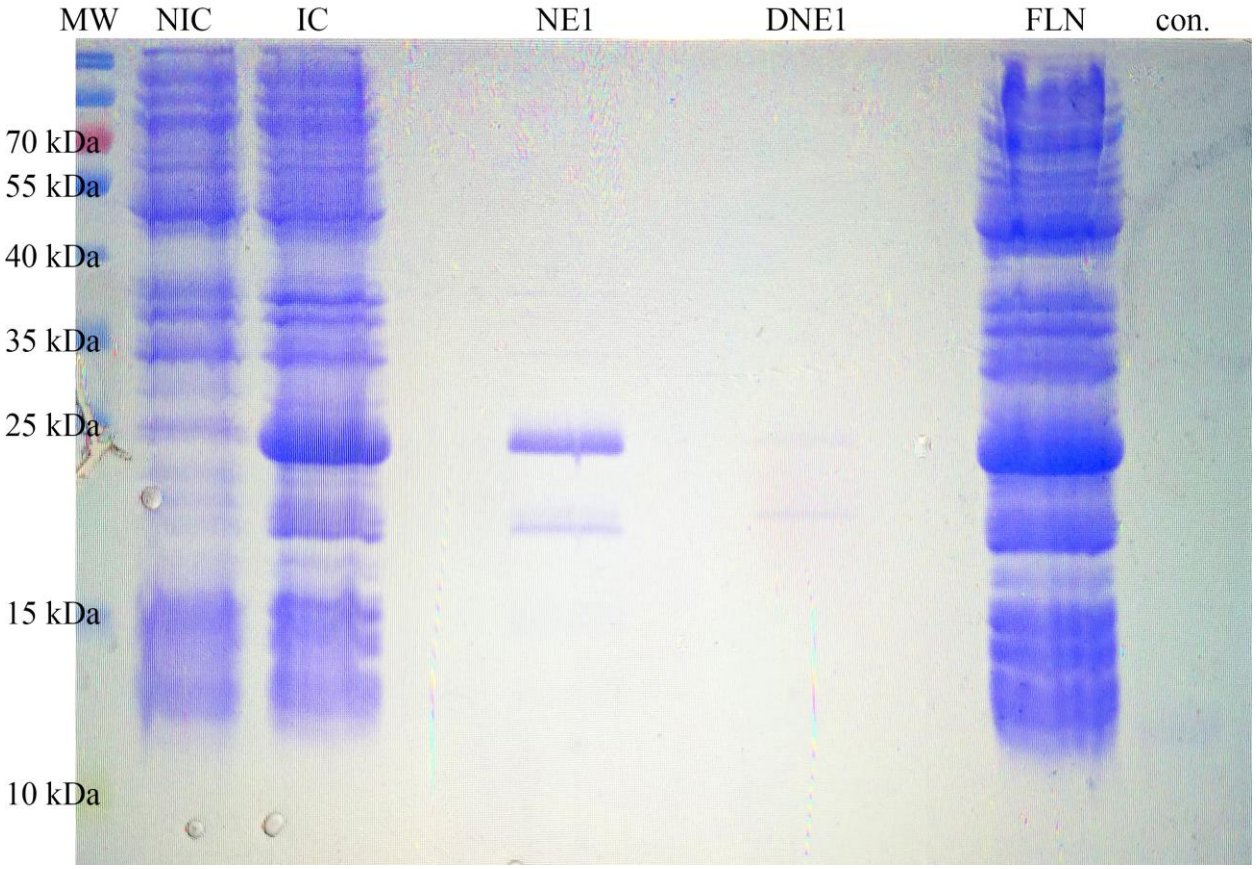

Figure 3.1.6 Analysis of the ULP1 Digest.
The ULP1 digested sample (DNE1) is observed at 25 kDa with a reduced protein concertation after dialysis and digest.

Isolation of 6His-SMT3-CCL19$_{(8-83)}$ by Ni-NTA Magnetic Beads

Previous attempts to digest SMT3 with ULP1 failed due to protein loss, all previously isolated sample was lost in previous run as a small quantity of protein was isolated. A new protein sample was required and methods to increase protein concentration is required. A newly transformed culture of *E. coli* BL21(DE3) in TB media induced according to previous methods was prepared. The insoluble fraction was loaded into Ni-NTA magnetic beads, collected samples were analyzed by SDS-PAGE (Figure 3.1.7) using SYPRO Ruby due to the low protein concentration. The sample was quantified by BCA assay but fell below the minimum protein

standard resulting with negative values. Results show Ni-NTA magnetic beads are not efficient in protein capture, isolated protein was captured at a lower concentration than previous methods.

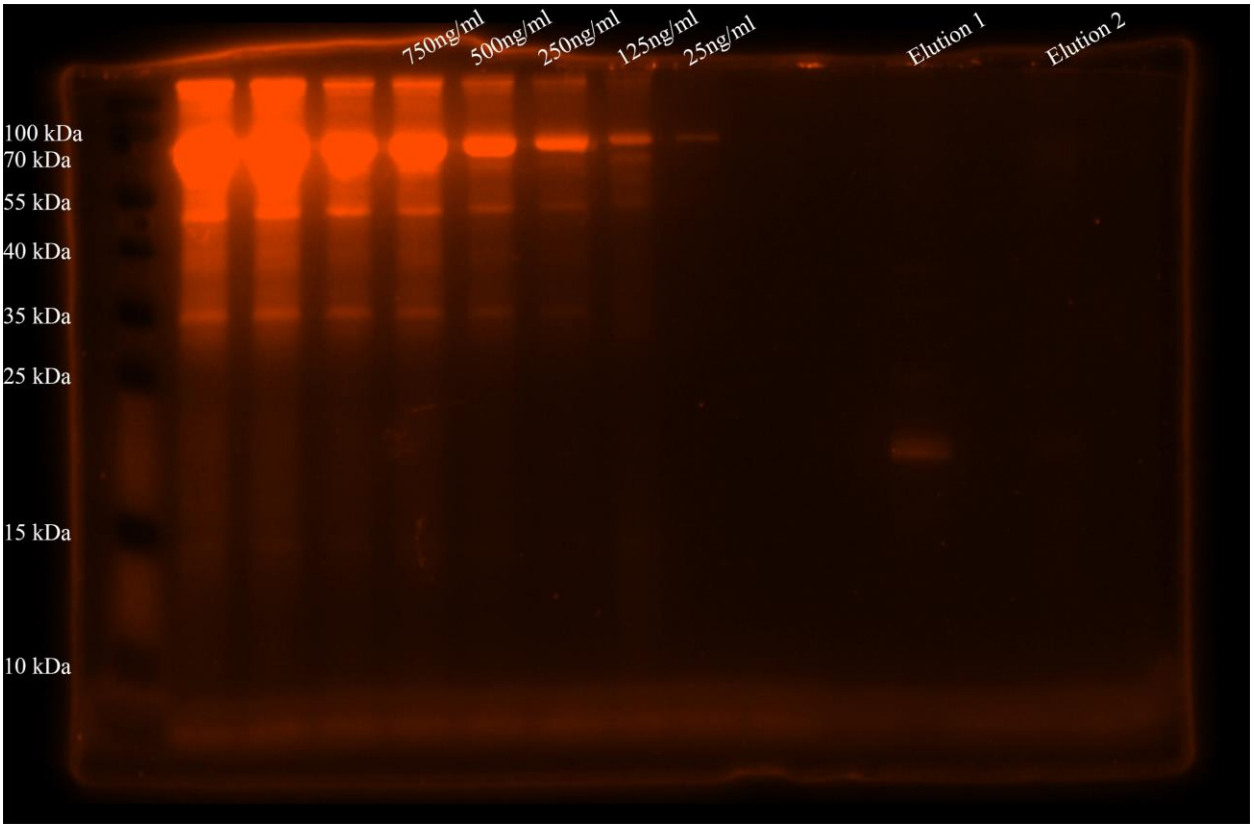

Figure 3.1.7 Analysis of Ni-NTA Magnetic Beads.
Using bovine serum albumin as a relative quantification method, a serial dilution of protein standards was included in the gel from 2,000 ng/mL – 25 ng/mL. The elution samples from magnetic beads are below 25 ng/mL, samples 1 and 2 exhibited a band below 25 kDa.

Upscaling Methods for Protein Expression and Isolation

Previous protein isolation methods did not produce significant quantities of fusion protein, upscaling methods are required. Confirmation of protein solubility was reassessed for upscaled protein expression methods using B-PER and analyzed by SDS-PAGE. Results show fusion protein is highly expressed in the insoluble fraction (Figure 3.1.8).

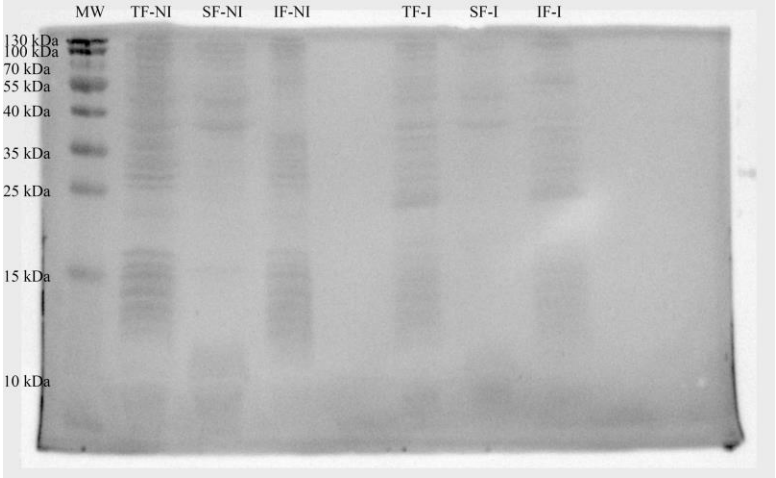

Figure 3.1.8 Analysis of B-PER Solubility Test.
Samples include Total Fraction (TF), Soluble Fraction (SF), Insoluble Fraction (IF), Not Induced (NI) and Induced (I). TF-NI compared to TF-Induced shows a solid band developed after induction around 25 kDa. Comparing induced soluble to insoluble we observe no band at 25 kDa for soluble but a solid band for insoluble.

A new culture in TB media was induced at a volume of 1 liter using standard methods. Using a different buffer composition and sample processing. The new buffer AD, as described in methods optimized sample lysis. The change in buffer extended lysis from approximately 5 minutes to 30 minutes. Increasing lysis' time was beneficial to avoid the protein degradation by heat in the sonicator. The insoluble fraction was prepared for isolation of fusion protein with a Ni-NTA Sepharose column (Cytiva) for FPLC (Cytiva). Once protein was loaded and bound to column the fusion protein underwent on-column refolding and continued to elution fractionation. The FPLC system analysis by UV-Vis showed a distinguished peak during elution gradient method (Figure 3.1.9). ÄKTA FPLC fractionation system elutes samples from A1-A12 continuing to the next alphabetical letter.

Figure 3.1.9 ÄKTA FPLC Ni-NTA Protein Purification Chromatogram.
Non-native 6His-SUMO-CCL198-83 purification blue line denotes UV absorbance at 280 nm, green line denotes concentration of imidazole.

Fractions in those peaks were analyzed by standard SDS-PAGE methods. Results show a distinguished band at ~25 kDa with some minor unknown contaminants (Figure 3.1.10A-D).

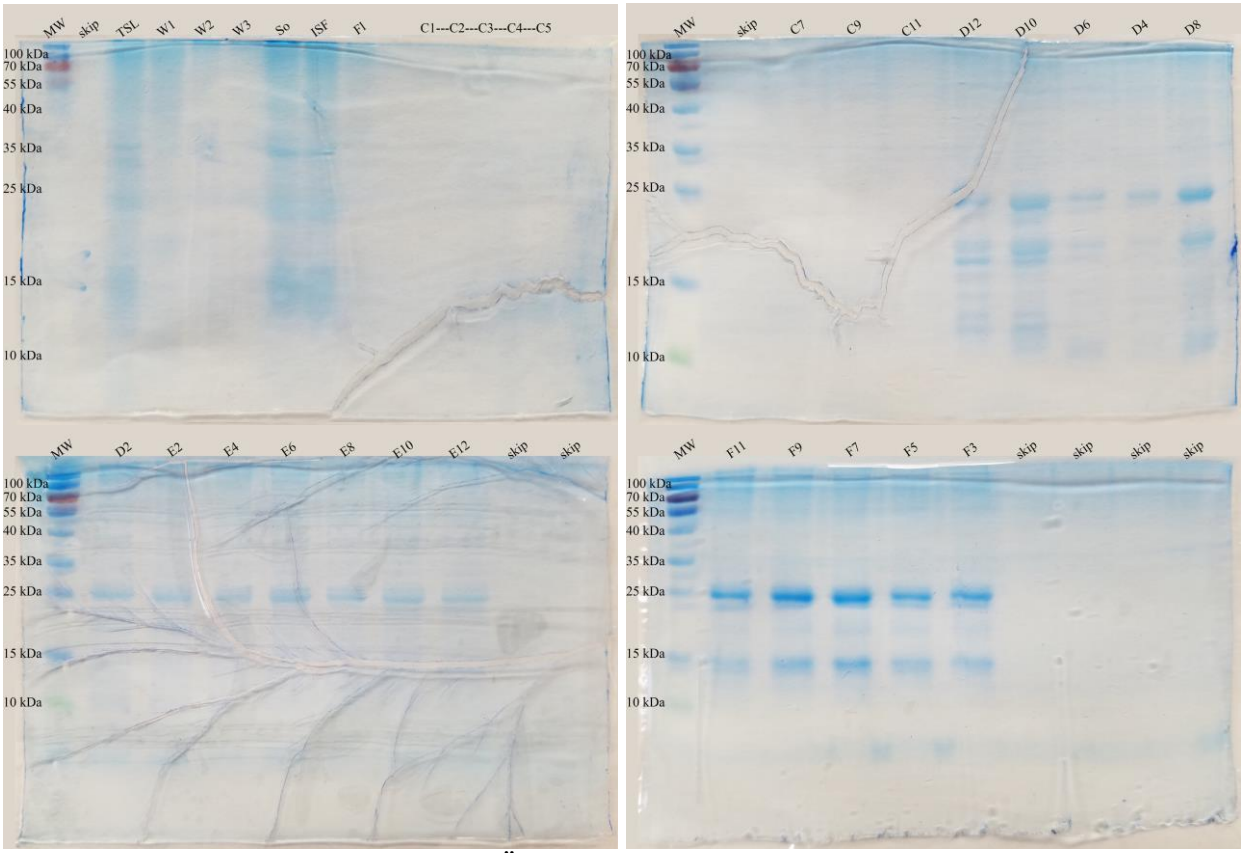

Figure 3.1.10A ÄKTA FPLC Ni-NTA SDS-PAGE

A) Analysis of elutions C1-C5, analysis of sample preparation during wash (W). B) Analysis of elutions C7-D8. C) Analysis of elutions D2-E12. D) Analysis of elutions F11-F3.

Samples were pooled together and concentrated using protein ultrafiltration and loaded into a Size Exclusion Column (SEC) 20 kDa (Cytiva) for buffer exchange and removal of unwanted proteins as an additional sample clean-up step. FPLC system shows a distinguished peak in UV-Vis analysis (Figure 3.1.11), indicative of the desired fusion protein.

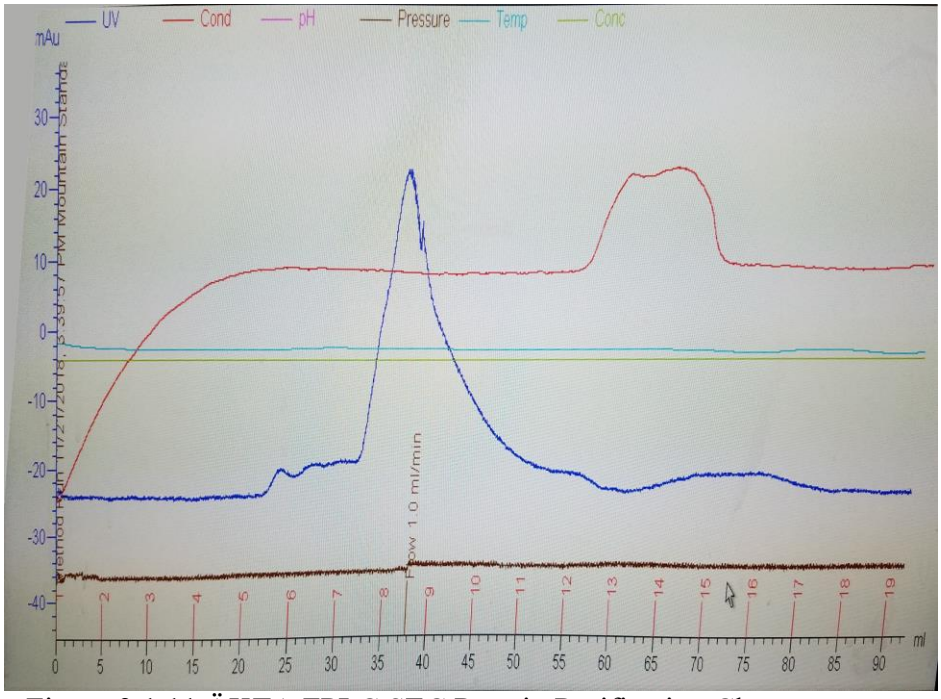

Figure 3.1.11 ÄKTA FPLC SEC Protein Purification Chromatogram. Chromatogram from size exclusion chromatography, blue line denotes UV absorbance at 280 nm, elution fractions shown below in red numbering.

Further analysis by SDS-PAGE reveals the UV peak is consistent with the expected molecular weight with a band observed at 25 kDa (Figure 3.1.12).

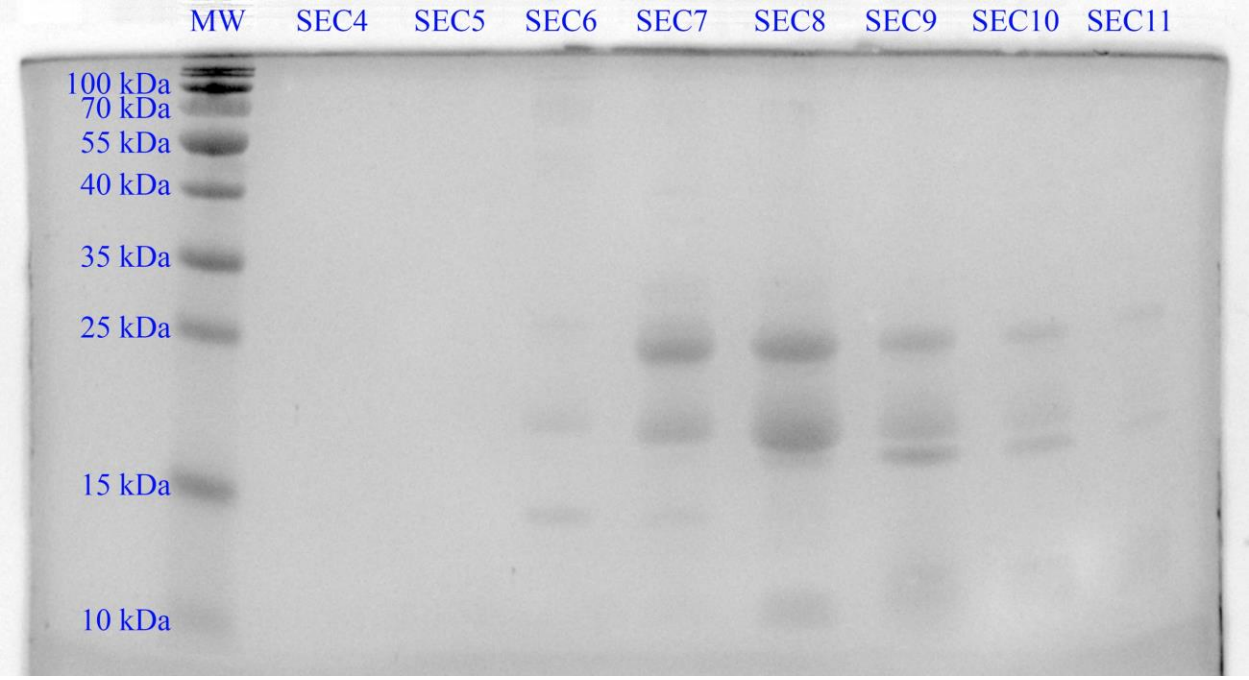

Figure 3.1.12 ÄKTA FPLC SEC SDS-PAGE Analysis S4-S11.
SDS gel analysis of fractions from size exclusion chromatography ÄKTA FPLC purification.

Fractions observed with the greatest protein concentration and purity were pooled together, concentrated using ultrafiltration and quantified using standard BCA assay methods.

Optimizing ULP1 Digest for 6His-SMT3-CCL19$_{(8-83)}$

A sample of isolated fusion protein was aliquoted (100 µg) and prepared for ULP1 digest for removal of SMT3. Analysis of digest by SDS-PAGE showed the ULP1 digest failed as the bands observed do not indicate any enzymatic activity (Figure 3.1.13).

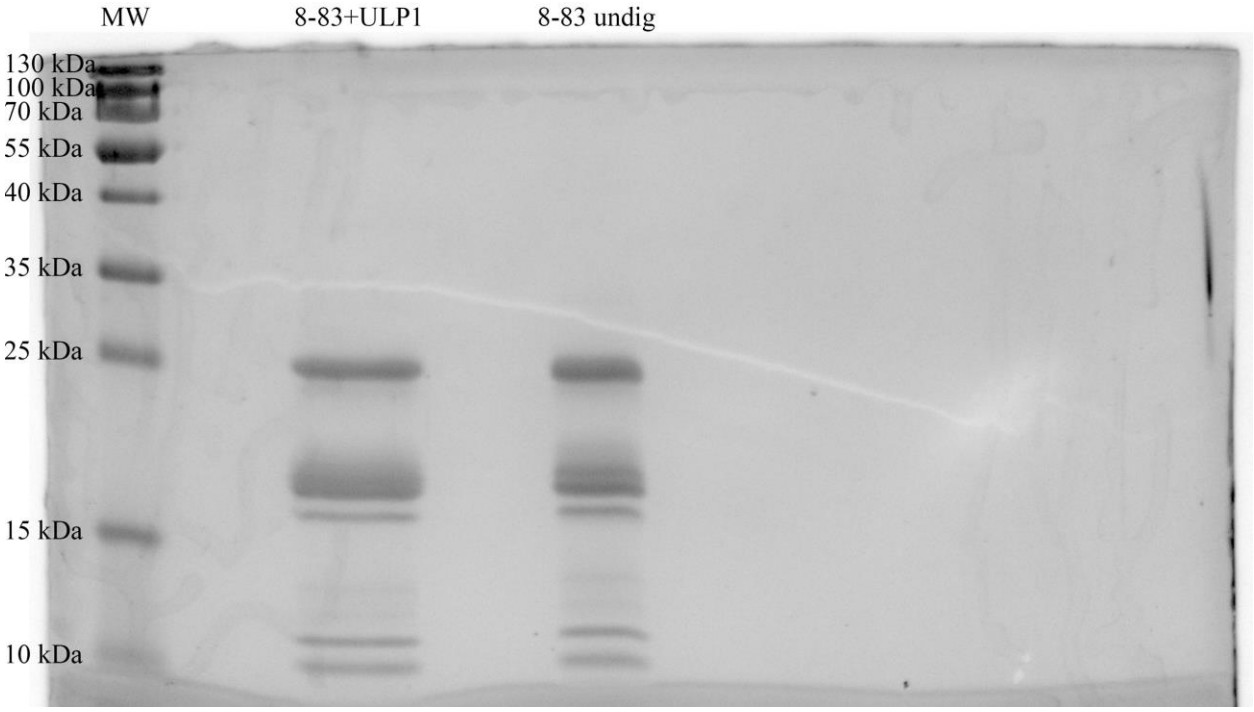

Figure 3.1.13 ULP1 Digest SDS Gel Analysis After SEC.
Analysis of the ULP1 samples, undigested fusion protein (8-83 undig) and experimental fusion protein digest (8-83+ULP1).

Testing for different conditions and buffer compositions begun to optimize the ULP1 digest. Test conditions included incubation time, incubation temperature, buffer composition, and ULP1 manufacturer. Multiple tests were completed (Table 3.1.1) the best conditions for ULP1 digest included a buffer composition with the addition of 1 mM DTT and 1 mM PMSF for enzymatic activity optimization, and the addition of 10 mM Cysteine and 0.5 mM Cystine to support chemokine fold via disulfide bonds formation. Analysis was completed by SDS-PAGE and western blotting for anti-CCL19 (Figure 3.1.14 and 3.1.15).

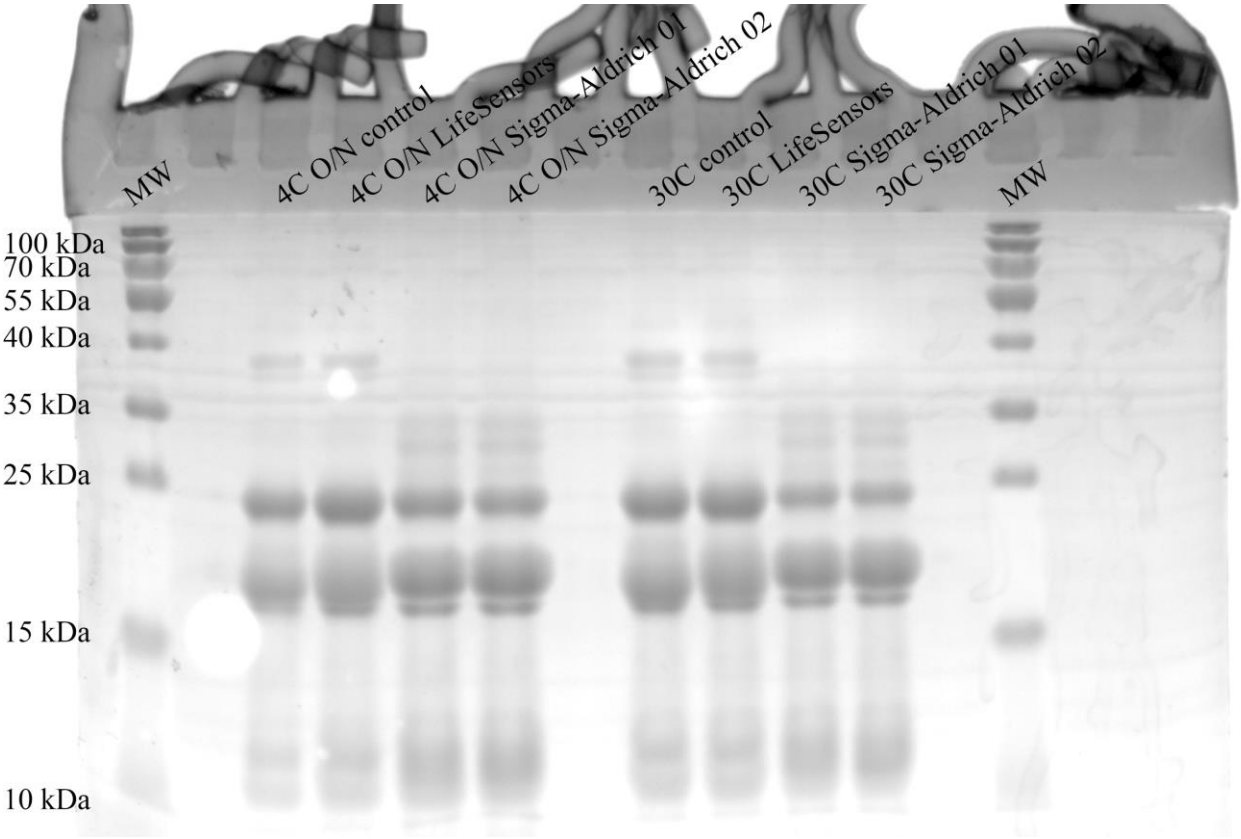

Figure 3.1.14 Optimization of the ULP1 Digest.
SDS gel analysis of experimental ULP1 digest conditions.

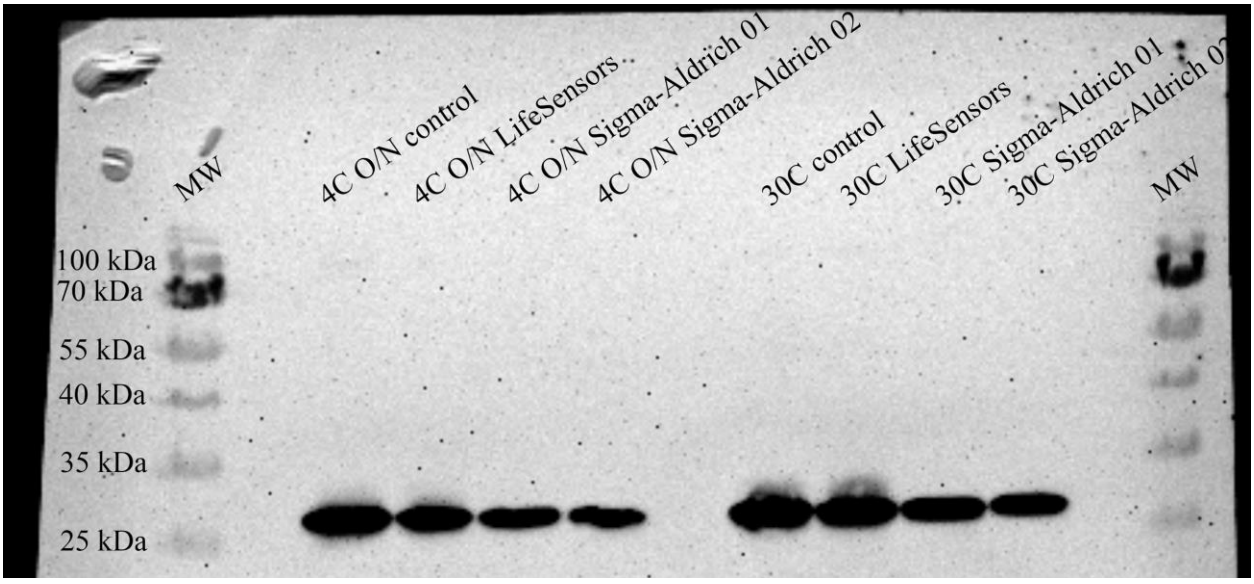

Figure 3.1.15 Optimized ULP1 Digest Western Blot
Western blot analysis with anti-CCL19 of experimental ULP1 digests.

Purification of CCL19$_{(8-83)}$ after ULP1 Digest

Data shows consistent and efficient ULP1 digest activity, the next step was the purification of the antagonist CCL19$_{(8-83)}$ from the byproducts of the digest. To achieve this, we completed anion exchange chromatography (AIEX) for the isolation of the antagonist based on protein charge dependent on pH. Using previously published works on the purification of chemokines we adapted a protocol using the same methods for working with SMT3 fusion proteins. At the correct buffer pH protein isolation is possible for the antagonist CCL19$_{(8-83)}$ from 6His-SMT3 and undigested fusion protein 6His-SMT3-CCL19$_{(8-83)}$. Completion of AIEX initially proved difficult as either the elution samples contained un-isolated CCL19$_{(8-83)}$ with digest byproducts or the undigested fusion protein, analysis by SDS-PAGE (Figure 3.1.16).

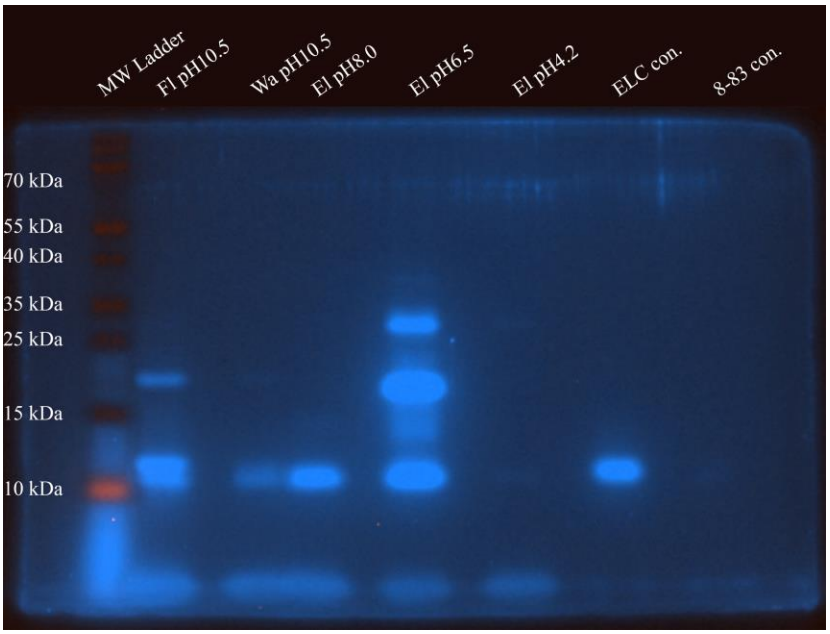

Figure 3.1.16 pH Based Elution for AIEX.
SDS gel analysis of fractions collected from AIEX based on pH.

Also due to the use of a high salt gradient in AIEX buffer exchange was required as any SDS-PAGE analysis would be skewed due to charge difference in samples. For this SPE was

completed on all samples obtained from AIEX using previous methods for SPE. This also had potential downfalls as SPE can lead to total sample loss or reduced protein recovery (Figure 3.1.17). Analyzing ion exchange chromatography samples proved difficult due to the high salt concentration. Analysis suggests samples containing Cysteine and Cystine (+Cys) in buffers was successful in recovering CCL19. Samples with +Cys do not exhibit a band in flowthrough or wash, elution sample exhibits one solid band at 10 kDa. Samples without Cysteine and Cystine (-Cys) did not exhibit a band for flowthrough, a band is observed at wash at 10 kDa, with possible protein aggregation observed for elution above 70 kDa

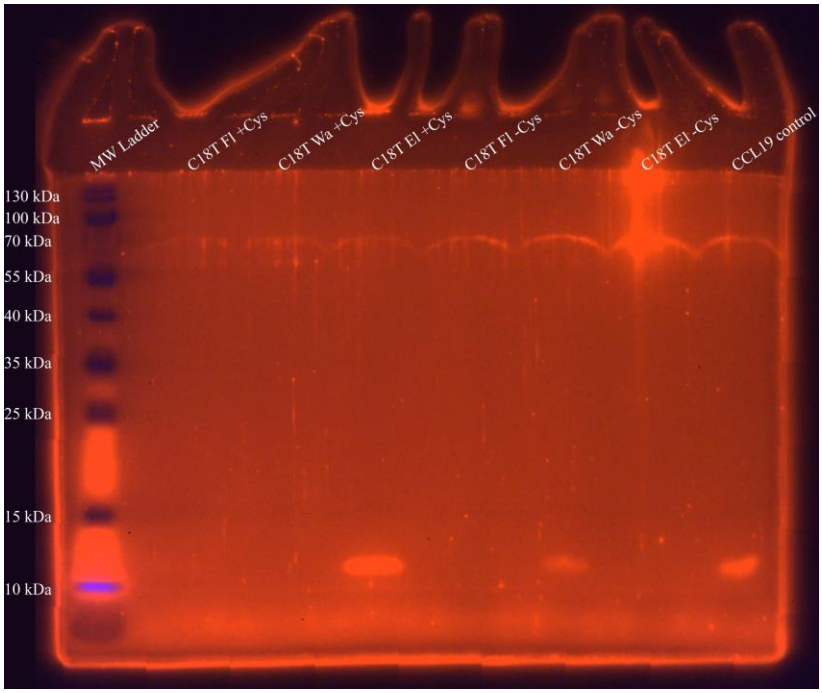

Figure 3.1.17 C18 Tips Sample Desalting Analysis.
SDS gel analysis of C18 Tips fractions comparison of cysteine addition.

Optimization was required for AIEX, multiple runs were completed using different buffer compositions and elution methods (Table 3.1.2). The elution methods were changed from pH dependent elution to salt concentration elution, pH dependent elution proved difficult due to buffer

diffusion equilibration. Salt dependent elution proved to be more consistent and reliable with the capability to be adapted for FPLC, allowing for automation and UV-Vis analysis during the purification. Analysis by SDS-PAGE and western blotting for anti-CCL19 and anti-SMT3 (Figure 3.1.18 and 3.1.19) suggested isolation of $CCL19_{(8\text{-}83)}$ was achieved.

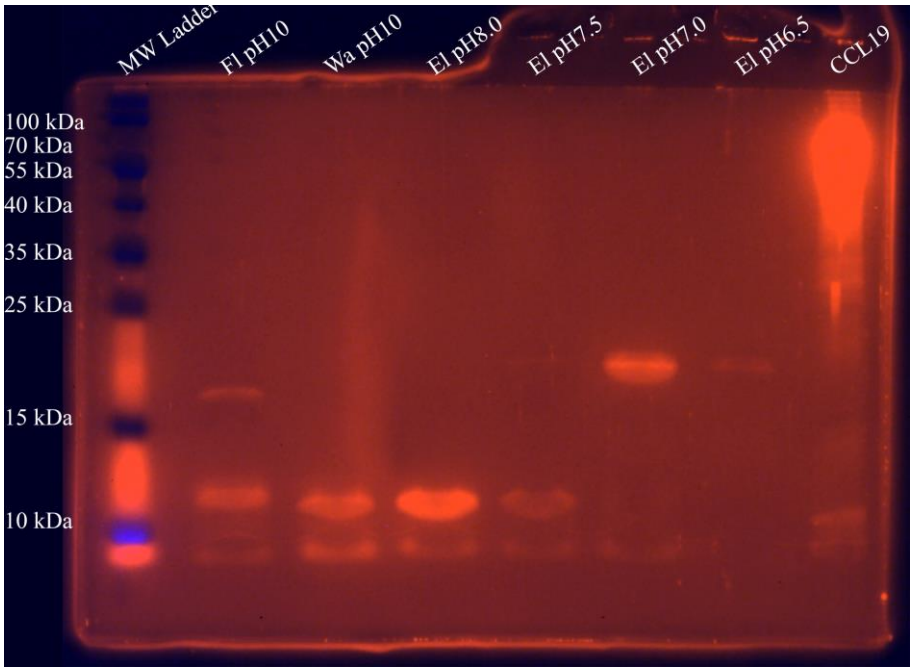

Figure 3.1.18 Salt Based Elution for AIEX
SDS gel analysis of AIEX using salt-based elution method.

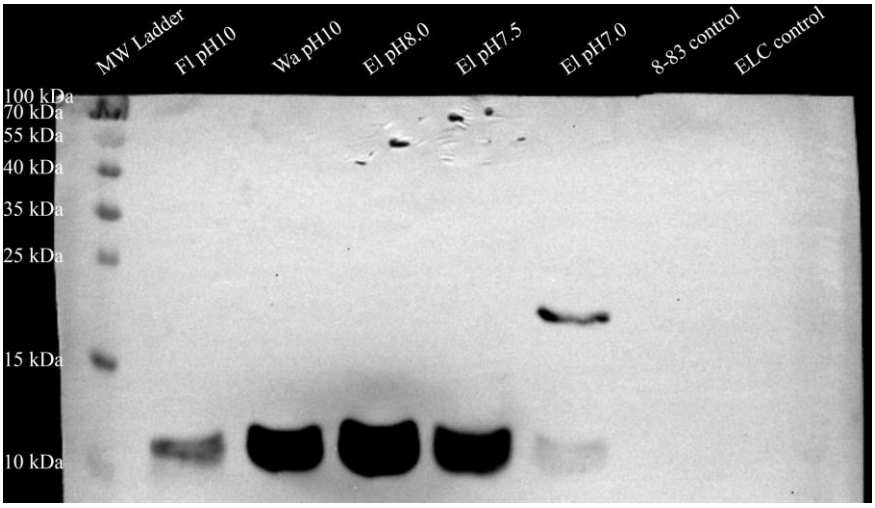

Figure 3.1.19 AIEX Western Blot for anti-CCL19
Western blot analysis of AIEX salt-based elution with anti-CCL19.

MALDI-TOF MS Analysis

Based on the previous data, further confirmation of purification and isolation of $CCL19_{(8-83)}$ was required. We quantified the total protein concentration using standard BCA assay and purified 80 µg of the isolated protein using Pierce C-18 Tips (for sample clean-up) prior to MALDI-TOF MS analysis. The sample was directly eluted into the Fleximass-DS polymeric plate and was allowed to evaporate. The completed analysis suggested that the isolated protein is inconsistent with the expected monoisotopic mass of 8,538.55 Da, we obtained a mass of 10, 559.20 Da with a two-charge variant at 5,288.77 Da (Figure 3.1.20).

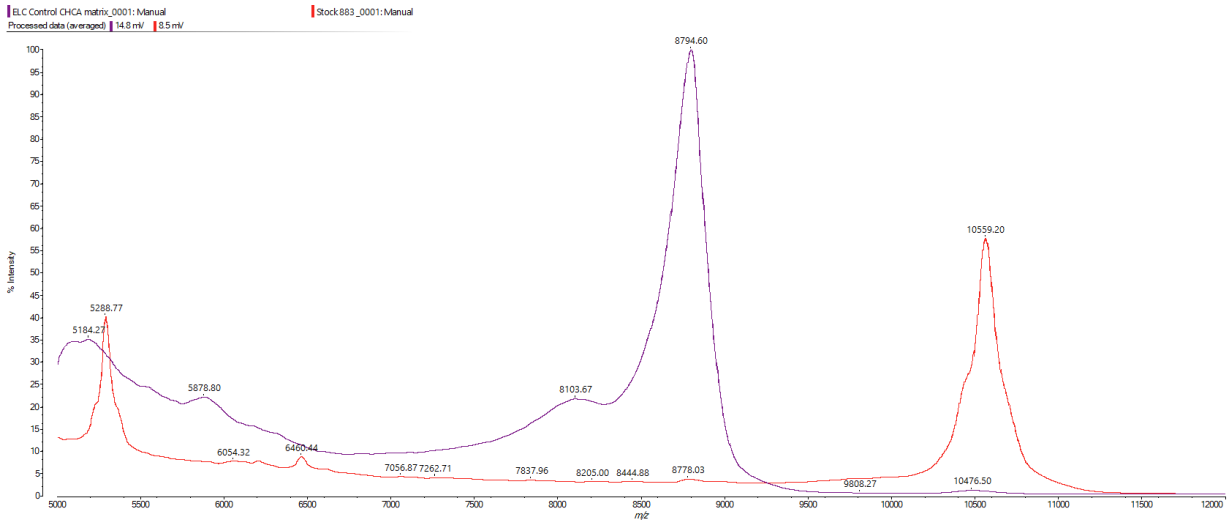

Figure 3.1.20 MALDI-TOF MS Sample Analysis
MALDI-TOF analysis of the AIEX elution fraction (purple), using hCCL19 as a control sample (orange).

3.1.4 Discussion

With the previous failed production of $CCL19_{(8-83)}$ confirmation of the plasmid construct was conducted. Bacterial transformation using *E. coli.* strain DH5α and pSUMO-$CCL19_{(8-83)}$ was grown in LB media culture, following culture growth a plasmid isolation was completed. Using a QIAGEN QIAprep Spin Miniprep kit the plasmid was isolated from the grown transformed bacterial culture. Isolated plasmid was quantified using Thermo Scientific NanoDrop to obtain a

plasmid purity ratios and plasmid concentration. Plasmid quantification proved sufficient quality and a plasmid double restriction digest was completed to assess plasmid identity and gene insert. Restriction enzymes BamHI and XhoI were used in single and double digest, analysis completed by inserting digested plasmid into an agarose gel. Using an E-Gel™ Agarose Gels with SYBR™ Safe DNA Gel Stain, 2% (Invitrogen) and E-Gel™ Power Snap Electrophoresis Device (Invitrogen) for rapid analysis of the digest plasmid samples. The plasmid digest analysis showed the correct approximate digest products (Figure 3.1.21), and the plasmid was sent for DNA sequencing. For plasmid DNA sequencing the T7 promotor primer sequence was used (T7: 5′-TAATACGACTCACTATAGGG- 3′). The sequenced data was analyzed using the UniProt BLAST Nucleotide tool with the UniProtKB reference proteomes + Swiss-Prot database and assessed for the expressed protein sequence[65]. The returned DNA sequence for pSUMO-CCL19$_{(8-83)}$ plasmid shows the mCCL19 gene is fully identified, although due to the multiple cloning sites additional amino acids were also expressed and with an additional C-terminus 6-His tag. (Figure 3.1.22 and 3.1.23). Previous western blot data has confirmed the presence of 6His-SUMO and CCL19 in the bacterial expression system (Figure 3.1.24). Also, western blot data of ULP1 digested samples and standard SDS gel analysis has shown the digested product in comparison to control hCCL19 is observed at a greater molecular weight. Based on the full DNA sequence analysis the plasmid needs modification for insertion of a stop sequence after the final amino acid for the antagonist CCL19$_{(8-83)}$. As previously mentioned, the C-terminus tail in the ligand plays an important role in the signaling pathway of CCR7. Hence, we do not want to include any modifications from the original identified antagonist. Reassessment of the plasmid should be conducted and perhaps modifying the expression system for a more suitable stable expression.

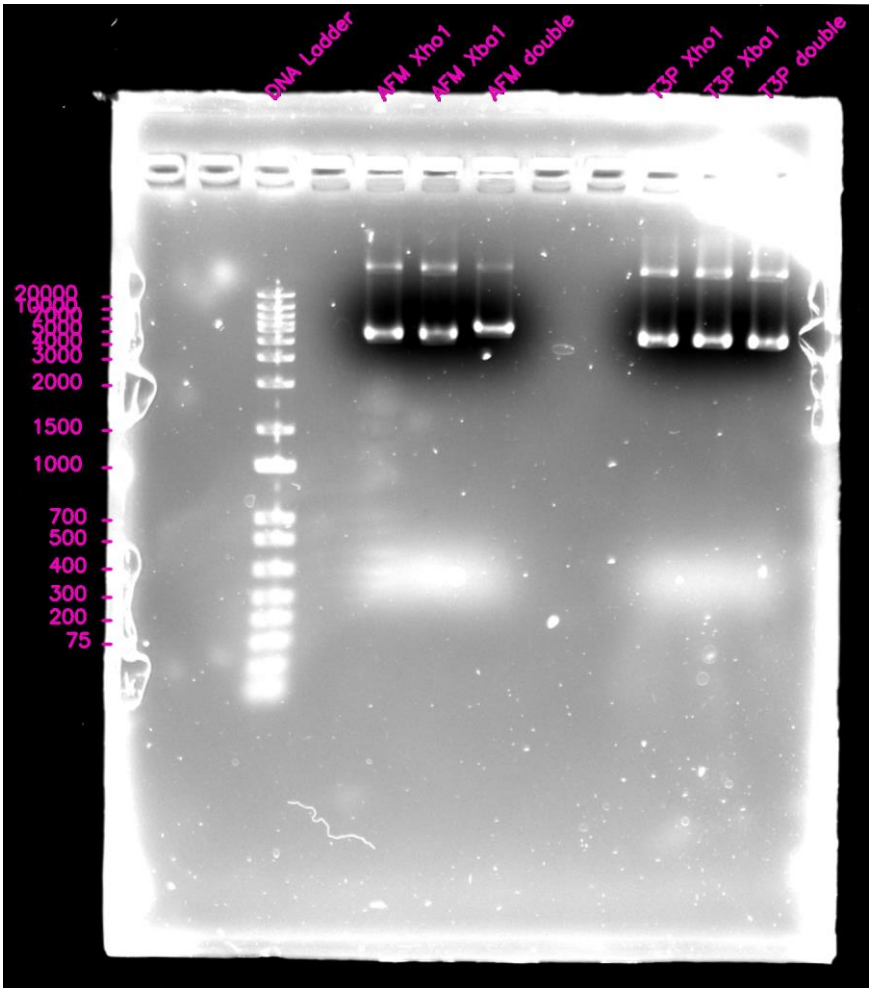

Figure 3.1.21 DNA Double Digest Analysis.
Isolated plasmid was digested with enzymes XhoI and XbaI, in single, single, and double digest for plasmid diagnostic identification.

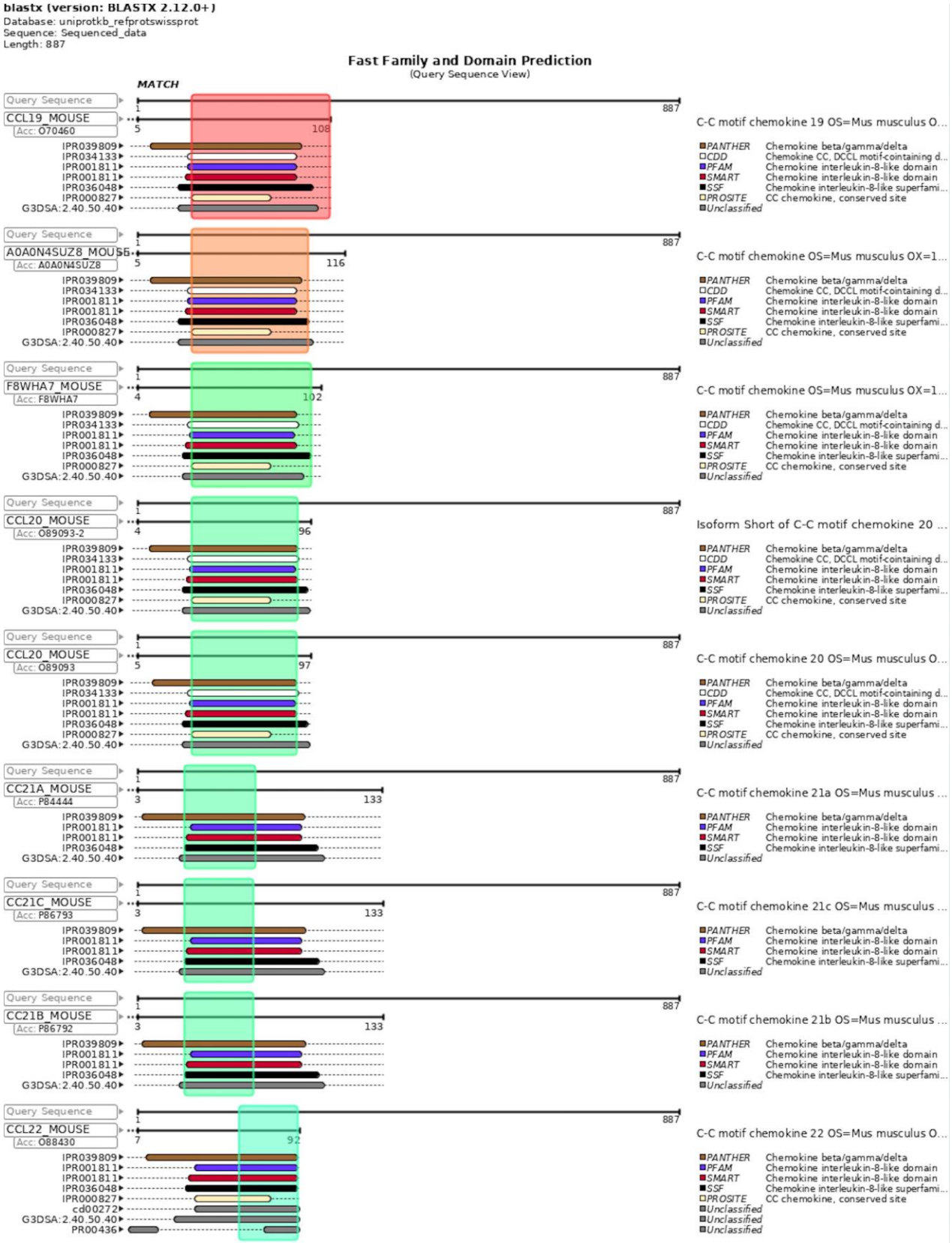

Figure 3.1.23 Sequence Analysis of Plasmid

Returned plasmid sequence analyzed by UniProt BLAST tool with restriction by taxonomy to

Mus musculus (Taxon ID 10090).

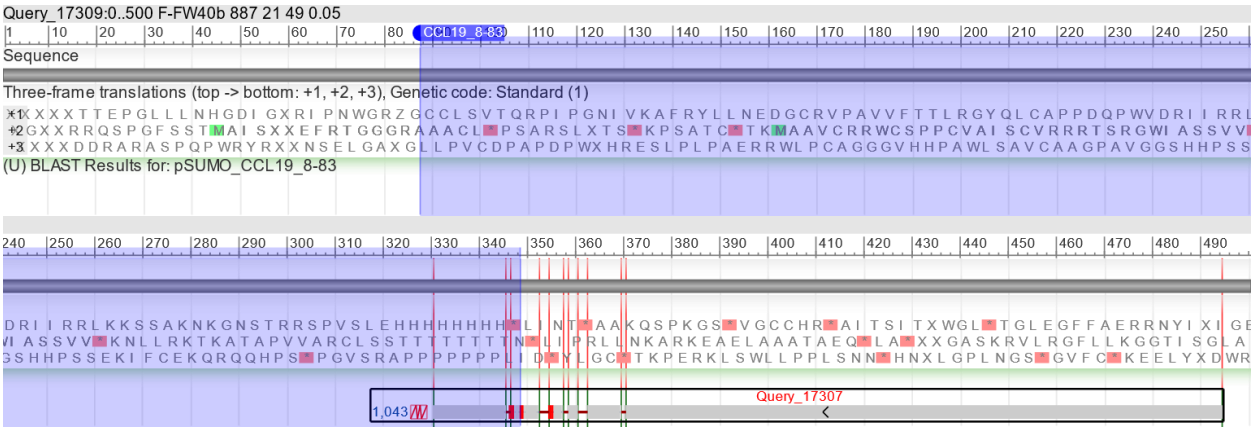

Figure 3.1.22 Sequence Analysis for Translation and Alignment.
Sequenced data analyzed with NIH Blast blastn Tool. The sequenced data was aligned to the original plasmid construct design. Three-frame translation was completed for the returned sequenced data.

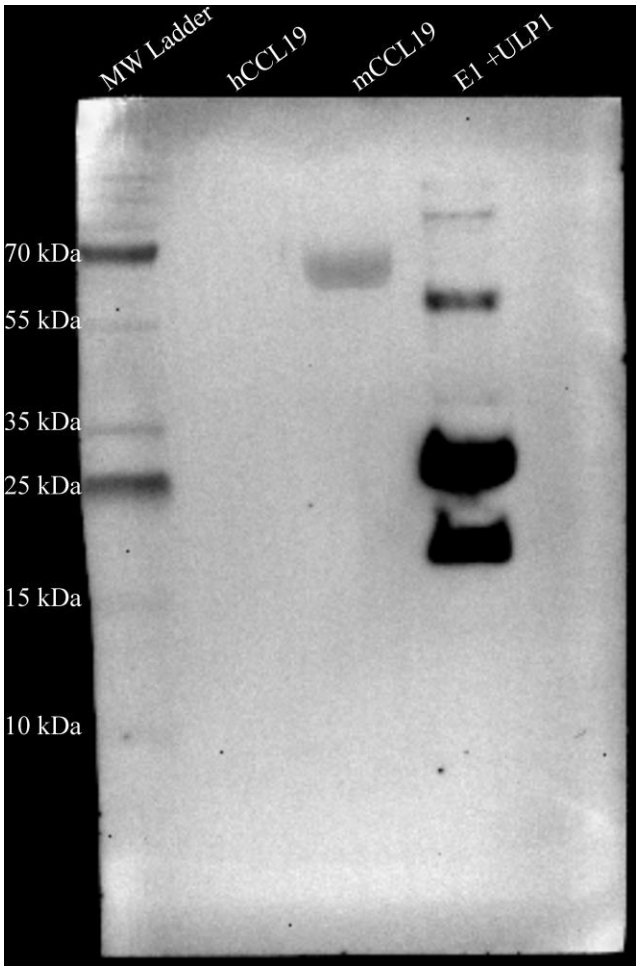

Figure 3.1.24 Western Blot Analysis for SUMO
Western blot analysis of isolated sample from AIEX elution (E1+ULP1) and controls for CCL19, using anti-SUMO (Yeast).

Chapter 4: Conclusions

4.1.1 Antagonizing CCR7 with $CCL19_{8-83}$ is a potential Therapeutic Agent for T-ALL

The CCR7 receptor although evolved to adapt and develop the human immune system is also involved in disease progression and can increase the rate of pathogenicity of other diseases when expressed in those specific cells. Its coaxes with CCL19 are for development of an immune response but has also been observed in disease development such as T-ALL CNS involvement[52]. T-ALL cells are demonstrated to be transported by CCR7 to the CNS; this appears to be due to the expression of the CCR7 ligand CCL19 on brain endothelial cells. Human tumors with Notch1-activating mutations express the Ccr7 gene, which is regulated by the T-ALL oncogene Notch1 activity. Despite its clinical significance, little is understood about the mechanism of leukemic cell infiltration into the CNS, which puts T-ALL patients at an elevated risk of CNS relapse. Thus, targeting CCR7 may present a treatment strategy to help T-ALL patients avoid CNS recurrence. The intensity of CNS-targeted therapy may be lowered through targeted suppression of CNS involvement in T-ALL, which would lessen the short- and long-term problems it is linked with. Current methods of production of the antagonist $CCL19_{8-83}$ are costly and as any production of protein production synthetically can be prone to multiple errors. Due to the size of the protein, 76AA long, many protein synthesizing manufacturers do not want to take on the task of creating it. Hence, this project explored alternatives in production of the antagonist by using current methods of chemokine purification like the SUMO expression method. The result in this project did not have the correct protein purified but shows the methods to obtain and produce mass quantities of this antagonists. The methods used here can be upscaled for increased production using bioreactors in the culturing of either bacterial or mammalian expression methods once small-

scale test systems are confirmed. This will allow for decreased cost and a reliable source of the antagonist in compliance with cGMP.

Designing a new expression plasmid with a de novo DNA sequence for the antagonist is highly recommended. Using Themo Fisher GeneArt services, a new expression system has been designed and optimized for mammalian protein expression. Using their de novo DNA tool the following construct was created, IgkH-8His-SMT3-CCL19$_{(8\text{-}83)}$ (Figure S1.1.2). Ig kappa chain V-III region VG precursor (IgkH) is modified signal peptide to secrete proteins in cells derived from different mammalian species[66]. The included 8-His tag will allow for IMAC isolation from the media once secreted from the mammalian cells. The mammalian cells for this expression method of choice are Expi293F human cells derived from the 293-cell line. They are maintained in suspension culture and will grow to high density in Expi293 Expression Medium. Continuing with the use of the SUMO expression method to ensure native N-terminus upon cleavage of the purification tag and to assist the proper protein folding to tertiary structure. This method will allow for a reliable source of functional antagonist, considering the mammalian expression system is more appropriate as we are working with a mammalian expressed protein. Utilizing mammalian cells assures appropriate post-translational changes, such as disulfide bonds and glycosylation, which can be crucial for precise functional research. One potential downside of this method is the initial monetary cost as research work with Expi293F cells and all its required reagents/media are expensive.

Further work can also be completed in attempts to purify the antagonists using a more suitable bacterial expression system such as newer generation of BL21(DE3) derivatives like Rosetta-gami B(DE3)pLysS. These cells boost both the expression of eukaryotic proteins and the creation of target protein disulfide bonds in the bacterial cytoplasm by combining the key

characteristics of BL21 (and its Tuner variant), Origami, and Rosetta. Also, with a re-engineered plasmid including only SMT3 and the exact sequence for the antagonist with no extra amino acids in the C-terminus. This system will allow production of the antagonist with a higher chance for protein stability and folding in a bacterial expression method, and a better cost of production.

This antagonist as shown here has an immense potential for preclinical trials using mouse models of T-ALL such as the inducible expression of [ROSA26 Floxed-stop Prdm14 (R26PR)] mice[67]. This mouse was engineered by targeting Floxed stop Prdm14 to the constitutive ROSA26 locus and breeding to Cre-recombinase transgenic lines. When R26PR is crossed with a Cre transgenic Mx1-Cre and induced with polyinosinic-polycytidylic acid (pIpC), mice develop early-onset T-cell acute lymphoblastic leukemia (T-ALL) with median overall survival of 41 days. The work here by completed and assessed by synthetic $CCL19_{(8\text{-}83)}$ has shown the need for further research and potential applications for multiple other studies due to the antagonistic properties.

Social, Biological and Pathological Implications

Insight regarding the mechanisms of action and responses of CCR7 and CCL19 ligation is important and necessary research in molecular biology. It has an enormous value regarding investigation of both biological and pathological areas that affect human conditions such as cancer. The homeostatic chemokine CCL19 is implicated as a mediator of tissue inflammation which is highly associated with cancer development. CCL19 can be used as a biomarker for a variety of illnesses, advancing prevention and individual patient assessment and treatment for diseases such as T cell acute lymphoblastic leukemia (T-ALL). The most recent worldwide and devastating COVID19 pandemic and its complications were associated with acute respiratory distress syndrome (ARDs) driven by hyperinflammation. Recent advances in research on

expression levels of cytokines and chemokines such CCL19 are crucial for patient outcomes. Previous knowledge in preclinical animal models suggested an elevation of the chemokine associated with SARS-CoV. A recent study with a 41-patient cohort recruited from ages of 18-59 years old, 44 cytokines were screened and identified that higher levels of CCL19 were associated with worse outcome disease outcome for COVID19-ARDS[68]. This research has useful applications in patient screening and their unique treatment.

CCL19 is critical in regulating DC and T cells; therefore, the immune response. This immunomodulatory molecule could be use in vaccine development against cancer. Recently the expression of proteins found only on cancerous cells (tumor antigens) along molecules such as CCL19 has being suggested as a strategy in DNA vaccination. The use of CCL19 as an adjuvant for vaccine development could potentially be use for enhancement of antitumor immune response. This effect of augmentation of the antitumor immunity was observed in preclinical *in vivo* trials with C57BL/6 mouse model. In the study an increase in CD8+ T-cell recruitment was observed[69].

Furthermore, as we suggest in our study the purification of an easily accessible, cost effective and functional folded antagonist is essential for treatment by preventing the binding of CCL19 to CCR7. In cancer CCL19 dysregulation is involved in breast, colorectal, lung cancer and leukemia as CCR7-CCL19 binding triggers the activates several pathways such as P13K/Akt, Rho-ROCK/MLC and ERK1-2-SAPK[70]. At present, higher expression of CCL19 is also considered a tumor biomarker for both diagnosis and prognosis[71]. It can also be used for therapy and disease management as a tumor suppressor activating anti-tumor immune responses. In cancer pathways involving Tyrosine receptors such as VEGFR (Vascular Endothelial Growth Factor Receptor), CCL19 prevents the proliferation of migration of the cancer cells[70]. The

phosphorylation of the amino acid tyrosine activates the VEGFR. The stimulation of the receptor leads to angiogenesis which is the formation of new blood vessels through which cancer cells once they lose their contact of inhibition can migrate to other parts of the body, such as the brain culminating in metastasis. Also, angiogenesis promotes tumor growth by supplying the cancer cells with oxygen and nutrients to sustain themselves, thrive and replicate. However, CCL19 can promote tumor variability from the original tumor since it is used as a maintenance treatment in leukemia treatments, the prolonged treatment can make tumors diversify from one another creating resistance (Figure 4.1.1).

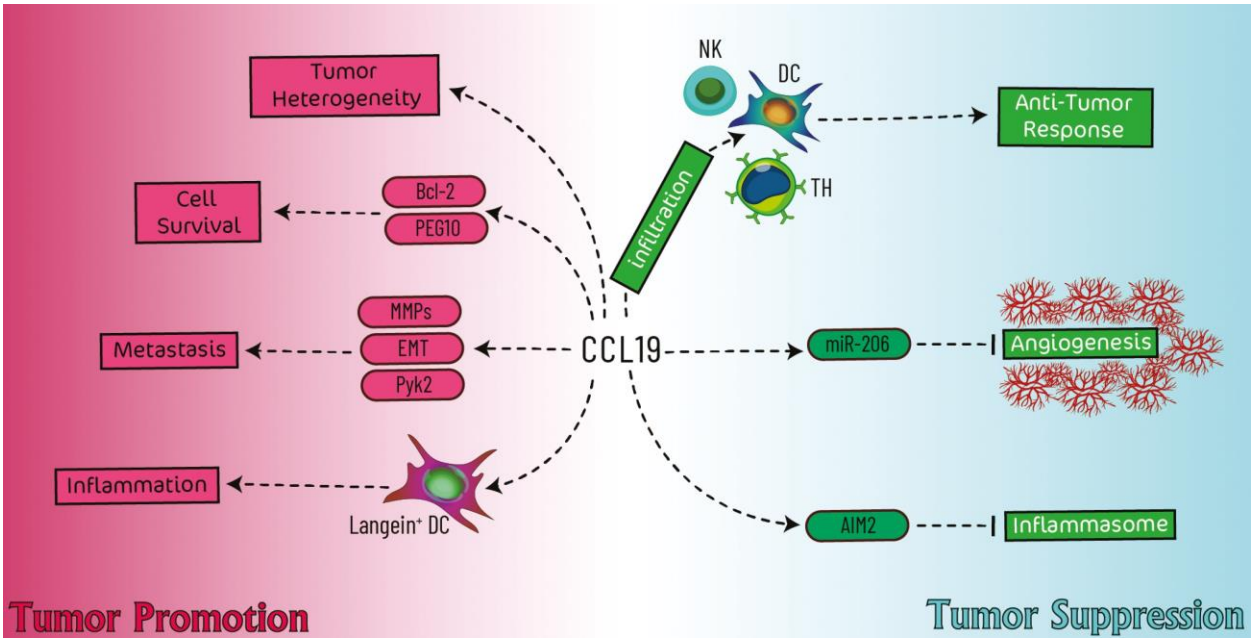

Figure 4.1.1 Schematic illustration of CCL19's involvement in cancer development. The tumor-suppressive role of CCL19 (shown in the blue area) relies on the enhancement of anti-tumor responses and inhibition of angiogenesis. In contrast, the tumor-promoting role of CCL19 (shown in the red area) is attributed to the inhibition of cell apoptosis, promotion of metastasis and tumor heterogeneity, and inflammation[70].

Consequently, the human and health impact that investigation on proteins such as CCL19 can lead our society in finding better treatments. Therapies specialized to patients in the

diverse pathogenesis of several diseases such as coronary artery disease, viral infection such as COVID19, HIV-Infection, and autoimmune disorders[72] are the future. This can revolutionize medicine, human care, consciousness of the importance of knowledge in our society for health practitioners, patients, decision making public and their representatives, leading us to a novel future. As our society, economic and political system is based on elected officials, the understanding of molecular biology can enlighten our leaders in objective and necessary science funding and its use by analyzing supported evidence. At present, the financing in scientific research is selected by biased governments; however, an improvement of the understanding of our body processes to the public can persuade them in taking careful consideration when electing representatives that will support the research that can benefit every social class in our society. As an example, the development of vaccines against cancer is crucial as every human being has the potential risk of developing a type of cancer. The research in CCL19 as a prognosis biomarker during COVID19 could have led to better distribution of the patient's treatment and assessment [68]. This highlights the importance of molecular biology in the assessment of patient care and treatment. This research could have been used in the evaluation or triage of first urgent patient candidates in receiving oxygen an admittance into the hospital's intensive care unit.

In our research we strive to understand all the implications of CCL19 binding to receptor CCR7 and the potential inhibition using antagonist $CCL19_{(8\text{-}83)}$. We also want to purify a correct folded protein that can be easily produced and cost effective.

Supplemental Data

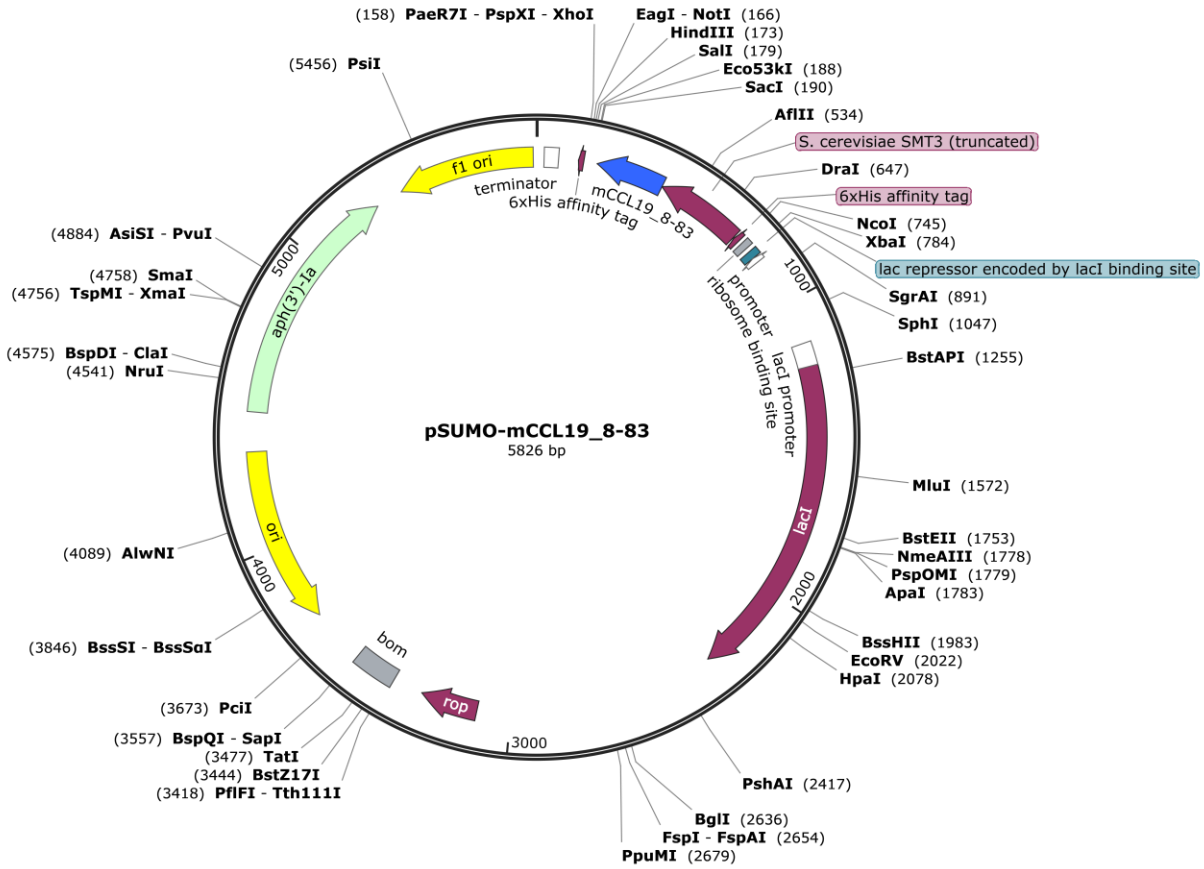

Figure S1.1.1 pSUMO-mCCL19$_{(8\text{-}83)}$ Plasmid Map

Plasmid map of pSUMO-Kan with gene insert mCCL19$_{(8\text{-}83)}$, inserted at the final amino acid of SMT3.

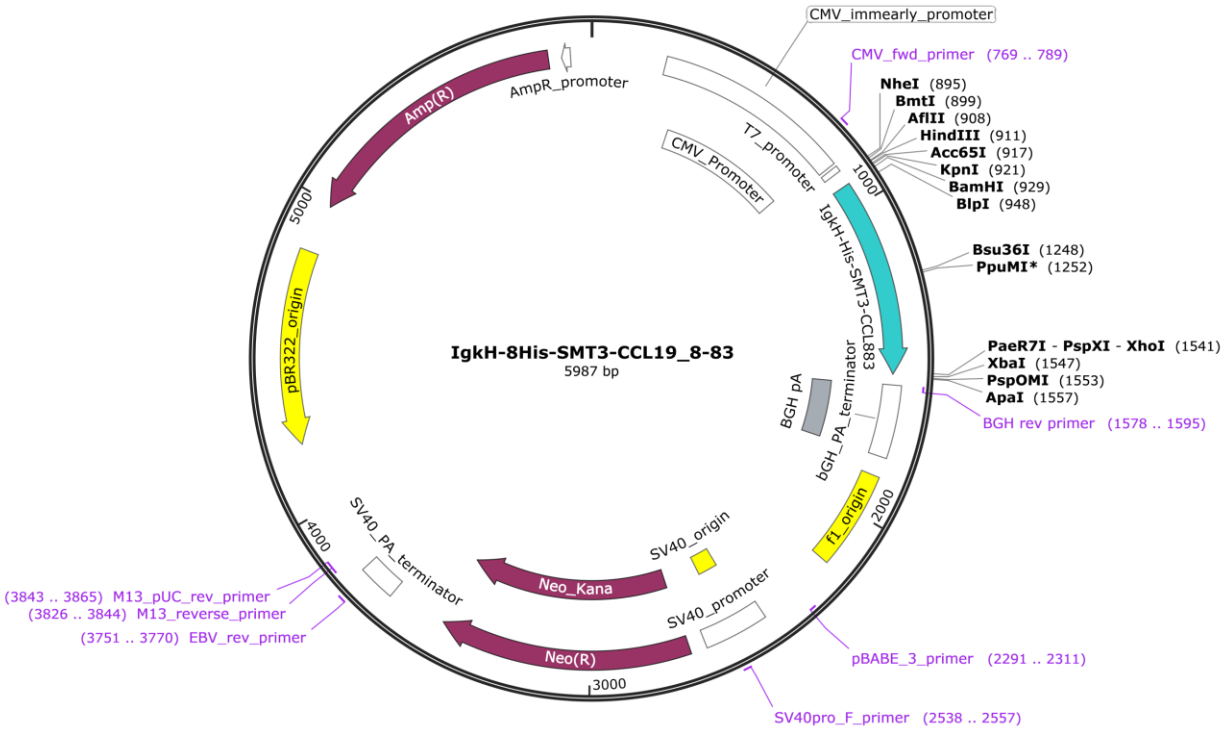

Figure S1.1.2 pcDNA 3.1 (+) IgkH-8His-SMT3-CCL19$_{(8\text{-}83)}$ Plasmid Map
Plasmid map of pcDNA 3.1 (+) with gene insert IgkH-8His-SMT3-mCCL19$_{(8\text{-}83)}$, designed using Thermo Scientific GeneArt services.

Table 3.1.1 ULP1 Protein Digest of CCL19$_{8\text{-}83}$ Fusion Protein Buffer Compositions

Digest Identifier	**Buffer Composition**	**pH**	**Incubation Time**	**Incubation Temperature**
A	100 mM Tris, 10 mM Cysteine, 0.5 mM Cystine.	8.0	48 hours	4°C
B	Refolding: 20 mM Tris, 150 mM NaCl, 1 mM EDTA, 1mM PMSF, 10 mM Cysteine, 0.5 mM Cystine, 10% Glycerol. Digest: 20 mM Tris, 150 mM NaCl, 1 mM EDTA, 1mM PMSF, 10% Glycerol.	8.5 8.5	16 hours 16 hours	4°C 4°C
C	20 mM Tris, 150 mM NaCl, 0.5 mM EDTA, 1mM PMSF.	7.4	16 hours	4°C
D	20 mM Tris, 150 mM NaCl, 2 mM DTT.	8.0	1 hour	30°C
E	Refolding: 50 mM Tris, 150 mM NaCl, 1 mM EDTA, 10 mM Cysteine, 0.5 mM Cystine, 10% Glycerol. Digest: 20 mM Tris, 1 mM EDTA, 10% Glycerol.	8.5 8.6	16 hours 16 hours	4°C 4°C

F	20 mM Tris, 150 mM NaCl, 0.5 mM EDTA, 1mM PMSF.	7.4	1 hour 16 hours	30°C 4°C
G	50 mM Tris, 150 mM NaCl, 1 mM EDTA, 2 mM DTT, 10 mM Cysteine, 0.5 mM Cystine, 10% Glycerol.	8.5	16 hours	4°C
H	50 mM Tris, 150 mM NaCl.	8.5	16 hours	4°C
I	50 mM Tris, 150 mM NaCl, 1 mM EDTA, 2 mM DTT, 10 mM Cysteine, 0.5 mM Cystine, 10% Glycerol, 1% Acetonitrile.	8.5	16 hours	4°C
J	50 mM Tris, 150 mM NaCl, 1% Acetonitrile	8.5	16 hours	4°C
K	50 mM Tris, 150 mM NaCl, 1 mM EDTA, 2 mM DTT, 10 mM Cysteine, 0.5 mM Cystine, 10% Glycerol, 5% Acetonitrile.	8.5	16 hours	4°C
L	50 mM Tris, 150 mM NaCl, 5% Acetonitrile.	8.5	16 hours	4°C
M	50 mM Tris, 150 mM NaCl, 2 mM DTT.	8.5	16 hours	4°C
N	50 mM Piperazine, 25 mM NaCl, 2 mM DTT, 10% Acetonitrile.	9.0	16 hours	4°C
O	50 mM Piperazine, 50 mM NaCl, 2 mM DTT, 5% Acetonitrile, 10% Glycerol.	10.0	16 hours	4°C
P	20 mM Piperazine, 100 mM NaCl, 10 mM Cysteine, 0.5 mM Cystine, 2 mM DTT, 2% Glycerol.	6.5	16 hours	4°C
Q	20 mM Piperazine, 100 mM NaCl, 10 mM Cysteine, 0.5 mM Cystine, 2 mM DTT, 2% Glycerol, 0.02% Tween-20.	6.5	16 hours	4°C
R	20 mM Piperazine, 100 mM NaCl, 10 mM Cysteine, 0.5 mM Cystine, 1 mM EDTA, 1 mM PMSF, 0.5 mM DTT, 2% Glycerol, 0.02% Tween-20.	8.0	16 hours	4°C
S	50 mM HEPES, 15 mM NaCl, 10 mM Cysteine, 0.5 mM Cystine, 1 mM EDTA, 1 mM PMSF, 0.5 mM DTT, 5% Glycerol, 0.05% Tween-20.	7.5	1 hour	37°C
T	20 mM Piperazine, 50 mM NaCl, 10 mM Cysteine, 0.5 mM Cystine, 1 mM EDTA, 1 mM PMSF, 0.5 mM DTT, 5% Glycerol, 0.05% Tween-20.	10.4	16 hours	4°C
U	Refolding: 100 mM Piperazine, 10 mM Cysteine, 0.5 mM Cystine, 1 mM EDTA, 1 mM PMSF. Digest: 100 mM Piperazine, 10 mM Cysteine, 0.5 mM Cystine	8.0 8.0	16 hours 16 hours	4°C 4°C

References

1. GPCR | Learn Science at Scitable. https://www.nature.com/scitable/topicpage/gpcr-14047471/.
2. Birkenbach, M., Josefsen, K., Yalamanchili, R., Lenoir, G. & Kieffl, E. Epstein-Barr virus-induced genes: first lymphocyte-specific G protein-coupled peptide receptors. *J Virol* **67**, 2209–2220 (1993).
3. Hauser, M. A. & Legler, D. F. Common and biased signaling pathways of the chemokine receptor CCR7 elicited by its ligands CCL19 and CCL21 in leukocytes. *J Leukoc Biol* **99**, 869–882 (2016).
4. Laufer, J. M., Kindinger, I., Artinger, M., Pauli, A. & Legler, D. F. CCR7 is recruited to the immunological synapse, acts as co-stimulatory molecule and drives LFA-1 clustering for efficient T cell adhesion through ZAP70. *Front Immunol* **10**, 3115 (2019).
5. Hauser, M. A. & Legler, D. F. Common and biased signaling pathways of the chemokine receptor CCR7 elicited by its ligands CCL19 and CCL21 in leukocytes. *J Leukoc Biol* **99**, 869–882 (2016).
6. Comerford, I. *et al.* A myriad of functions and complex regulation of the CCR7/CCL19/CCL21 chemokine axis in the adaptive immune system. *Cytokine Growth Factor Rev* **24**, 269–283 (2013).
7. Ohl, L. *et al.* CCR7 Governs Skin Dendritic Cell Migration under Inflammatory and Steady-State Conditions. *Immunity* **21**, 279–288 (2004).
8. Riol-Blanco, L. *et al.* The Chemokine Receptor CCR7 Activates in Dendritic Cells Two Signaling Modules That Independently Regulate Chemotaxis and Migratory Speed. *The Journal of Immunology* **174**, 4070–4080 (2005).
9. Iijima, N., Yanagawa, Y., Clingan, J. M. & Onoé, K. CCR7-mediated c-Jun N-terminal kinase activation regulates cell migration in mature dendritic cells. *Int Immunol* **17**, 1201–1212 (2005).
10. Hauser, M. A. & Legler, D. F. Common and biased signaling pathways of the chemokine receptor CCR7 elicited by its ligands CCL19 and CCL21 in leukocytes. *J Leukoc Biol* **99**, 869–882 (2016).
11. Bardi, G., Lipp, M., Baggiolini, M. & Loetscher, P. The T cell chemokine receptor CCR7 is internalized on stimulation with ELC, but not with SLC. doi:10.1002/1521-4141.
12. Laporte, S. A. *et al.* The β2-adrenergic receptor/βarrestin complex recruits the clathrin adaptor AP-2 during endocytosis. *Proc Natl Acad Sci U S A* **96**, 3712 (1999).
13. Dhyani, V. *et al.* GPCR mediated control of calcium dynamics: A systems perspective. *Cell Signal* **74**, 109717 (2020).
14. Kehrl, J. H. Chemoattractant receptor signaling and the control of lymphocyte migration. *Immunol Res* **34**, 211–227 (2006).
15. Human chemokines: An update - ProQuest. https://www.proquest.com/docview/201639244?pq-origsite=gscholar&fromopenview=true.
16. Sue Goo Rhee & Yun Soo Bae. Regulation of phosphoinositide-specific phospholipase C isozymes. *Journal of Biological Chemistry* **272**, 15045–15048 (1997).
17. Sankaran, B., Osterhout, J., Wu, D. & Smrcka, A. v. Identification of a structural element in Phospholipase C β2 that interacts with G protein βγ. *Journal of Biological Chemistry* **273**, 7148–7154 (1998).

18. Mandeville, J. T. H. & Maxfield, F. R. Effects of Buffering Intracellular Free Calcium on Neutrophil Migration Through Three-Dimensional Matrices. *J Cell Physiol* **171**, 168–178 (1997).
19. Stephens, L. *et al.* A novel phosphoinositide 3 kinase activity in myeloid-derived cells is activated by G protein βγ subunits. *Cell* **77**, 83–93 (1994).
20. Tilton, B. *et al.* Signal Transduction by Cxc Chemokine Receptor 4Stromal Cell–Derived Factor 1 Stimulates Prolonged Protein Kinase B and Extracellular Signal–Regulated Kinase 2 Activation in T Lymphocytes. *Journal of Experimental Medicine* **192**, 313–324 (2000).
21. Meili, R. *et al.* Chemoattractant-mediated transient activation and membrane localization of Akt/PKB is required for efficient chemotaxis to cAMP in Dictyostelium. *EMBO J* **18**, 2092–2105 (1999).
22. Servant, G. *et al.* Polarization of chemoattractant receptor signaling during neutrophil chemotaxis. *Science (1979)* **287**, 1037–1040 (2000).
23. Steen, A., Larsen, O., Thiele, S. & Rosenkilde, M. M. Biased and G protein-independent signaling of chemokine receptors. *Front Immunol* **5**, 277 (2014).
24. Jørgensen, A. S., Rosenkilde, M. M. & Hjortø, G. M. Biased signaling of G protein-coupled receptors – From a chemokine receptor CCR7 perspective. *Gen Comp Endocrinol* **258**, 4–14 (2018).
25. Jørgensen, A. S. *et al.* CCL19 with CCL21-tail displays enhanced glycosaminoglycan binding with retained chemotactic potency in dendritic cells. *J Leukoc Biol* **104**, 401–411 (2018).
26. Hjortø, G. M. *et al.* Differential CCR7 targeting in dendritic cells by three naturally occurring CC-chemokines. *Front Immunol* **7**, 568 (2016).
27. Zhiming, W., Luman, W., Tingting, Q. & Yiwei, C. Chemokines and receptors in intestinal B lymphocytes. *J Leukoc Biol* **103**, 807–819 (2018).
28. Raju, R. *et al.* Differential ligand-signaling network of CCL19/CCL21-CCR7 system. *Database* **2015**, 106 (2015).
29. Rot, A. & von Andrian, U. H. Chemokines in innate and adaptive host defense: basic chemokinese grammar for immune cells. *Annu Rev Immunol* **22**, 891–928 (2004).
30. Anderson, C. A., Solari, R. & Pease, J. E. Biased agonism at chemokine receptors: obstacles or opportunities for drug discovery? *J Leukoc Biol* **99**, 901–909 (2016).
31. Hjortø, G. M. *et al.* Differential CCR7 targeting in dendritic cells by three naturally occurring CC-chemokines. *Front Immunol* **7**, 568 (2016).
32. Förster, R., Davalos-Misslitz, A. C. & Rot, A. CCR7 and its ligands: balancing immunity and tolerance. *Nature Reviews Immunology 2008 8:5* **8**, 362–371 (2008).
33. Takahama, Y. Journey through the thymus: stromal guides for T-cell development and selection. *Nature Reviews Immunology 2006 6:2* **6**, 127–135 (2006).
34. Boyle, S. T. *et al.* The chemokine receptor CCR7 promotes mammary tumorigenesis through amplification of stem-like cells. *Oncogene 2016 35:1* **35**, 105–115 (2015).
35. Li, X. *et al.* Small molecule-mediated upregulation of CCR7 ameliorates murine experimental autoimmune encephalomyelitis by accelerating T-cell homing. *Int Immunopharmacol* **53**, 33–41 (2017).
36. Ortiz Zacarías, N. v., Bemelmans, M. P., Handel, T. M., de Visser, K. E. & Heitman, L. H. Anticancer opportunities at every stage of chemokine function. *Trends Pharmacol Sci* **42**, 912–928 (2021).

37. Pilkington, K. R., Clark-Lewis, I. & McColl, S. R. Inhibition of Generation of Cytotoxic T Lymphocyte Activity by a CCL19/Macrophage Inflammatory Protein (MIP)-3β Antagonist *. *Journal of Biological Chemistry* **279**, 40276–40282 (2004).
38. Veldkamp, C. T. *et al.* On-column refolding of recombinant chemokines for NMR studies and biological assays. *Protein Expr Purif* **52**, 202–209 (2007).
39. Ma, Y. *et al.* High Efficient Expression, Purification, and Functional Characterization of Native Human Epidermal Growth Factor in Escherichia coli. *Biomed Res Int* **2016**, (2016).
40. Veldkamp, C. T. *et al.* Production of recombinant chemokines and validation of refolding. *Methods Enzymol* **570**, 539 (2016).
41. Hendriks, I. A. & Vertegaal, A. C. O. A high-yield double-purification proteomics strategy for the identification of SUMO sites. *Nature Protocols 2016 11:9* **11**, 1630–1649 (2016).
42. Weeks, S. D., Drinker, M. & Loll, P. J. Ligation independent cloning vectors for expression of SUMO fusions. *Protein Expr Purif* **53**, 40–50 (2007).
43. Buonamici, S. *et al.* CCR7 signalling as an essential regulator of CNS infiltration in T-cell leukaemia. *Nature 2009 459:7249* **459**, 1000–1004 (2009).
44. Cannon, J. L., Oruganti, S. R. & Vidrine, D. W. Molecular regulation of T-ALL cell infiltration into the CNS. *Oncotarget* **8**, 84626 (2017).
45. Louveau, A. *et al.* CNS lymphatic drainage and neuroinflammation are regulated by meningeal lymphatic vasculature. *Nature Neuroscience 2018 21:10* **21**, 1380–1391 (2018).
46. van Vlierberghe, P. & Ferrando, A. The molecular basis of T cell acute lymphoblastic leukemia. *J Clin Invest* **122**, 3398–3406 (2012).
47. Pinto, I. *et al.* NRARP displays either pro- or anti-tumoral roles in T-cell acute lymphoblastic leukemia depending on Notch and Wnt signaling. *Oncogene 2019 39:5* **39**, 975–986 (2019).
48. Karrman, K. & Johansson, B. Pediatric T-cell acute lymphoblastic leukemia. *Genes Chromosomes Cancer* **56**, 89–116 (2017).
49. Litzow, M. R. & Ferrando, A. A. How I Treat How I treat T-cell acute lymphoblastic leukemia in adults. (2015) doi:10.1182/blood-2014-10-551895.
50. Belver, L. & Ferrando, A. The genetics and mechanisms of T cell acute lymphoblastic leukaemia. *Nature Reviews Cancer 2016 16:8* **16**, 494–507 (2016).
51. Hoelzer, D. & Gökbuget, N. T-Cell Lymphoblastic Lymphoma and T-Cell Acute Lymphoblastic Leukemia: A Separate Entity? *Clin Lymphoma Myeloma* **9**, S214–S221 (2009).
52. Buonamici, S. *et al.* CCR7 signalling as an essential regulator of CNS infiltration in T-cell leukaemia. *Nature 2009 459:7249* **459**, 1000–1004 (2009).
53. Hauser, M. A. *et al.* Distinct CCR7 glycosylation pattern shapes receptor signaling and endocytosis to modulate chemotactic responses. *J Leukoc Biol* **99**, 993–1007 (2016).
54. Nitta, T., Nitta, S., Yu, L., Lipp, M. & Takahama, Y. CCR7-mediated migration of developing thymocytes to the medulla is essential for negative selection to tissue-restricted antigens. *Proc Natl Acad Sci U S A* **106**, 17129–17133 (2009).
55. Bill, C. A. & Vines, C. M. Phospholipase C. *Adv Exp Med Biol* **1131**, 215–242 (2020).

56. Shannon, L. A., Calloway, P. A., Welch, T. P. & Vines, C. M. CCR7/CCL21 migration on fibronectin is mediated by phospholipase Cγ1 and ERK1/2 in primary T lymphocytes. *Journal of Biological Chemistry* **285**, 38781–38787 (2010).
57. Byers, M. A. *et al.* Arrestin 3 Mediates Endocytosis of CCR7 following Ligation of CCL19 but Not CCL21. *The Journal of Immunology* **181**, 4723–4732 (2008).
58. Veldkamp, C. T. *et al.* Solution Structure of CCL19 and Identification of Overlapping CCR7 and PSGL-1 Binding Sites. *Biochemistry* **54**, 4163–4166 (2015).
59. Yoshida, R. *et al.* Molecular Cloning of a Novel Human CC Chemokine EBI1-ligand Chemokine That Is a Specific Functional Ligand for EBI1, CCR7 *. *Journal of Biological Chemistry* **272**, 13803–13809 (1997).
60. Ott, T. R. *et al.* The N-terminal domain of CCL21 reconstitutes high affinity binding, G protein activation, and chemotactic activity, to the C-terminal domain of CCL19. *Biochem Biophys Res Commun* **348**, 1089–1093 (2006).
61. Ott, T. R. *et al.* Determinants of High-Affinity Binding and Receptor Activation in the N-Terminus of CCL-19 (MIP-3β). *Biochemistry* **43**, 3670–3678 (2004).
62. Veldkamp, C. T., Peterson, F. C., Pelzek, A. J. & Volkman, B. F. The monomer–dimer equilibrium of stromal cell-derived factor-1 (CXCL 12) is altered by pH, phosphate, sulfate, and heparin. *Protein Sci* **14**, 1071 (2005).
63. Marblestone, J. G. *et al.* Comparison of SUMO fusion technology with traditional gene fusion systems: Enhanced expression and solubility with SUMO. *Protein Science* **15**, 182–189 (2006).
64. Malakhov, M. P. *et al.* SUMO fusions and SUMO-specific protease for efficient expression and purification of proteins. *Journal of Structural and Functional Genomics 2004 5:1* **5**, 75–86 (2004).
65. Consortium, T. U. *et al.* UniProt: the Universal Protein Knowledgebase in 2023. *Nucleic Acids Res* **51**, D523–D531 (2023).
66. Attallah, C., Etcheverrigaray, M., Kratje, R. & Oggero, M. A highly efficient modified human serum albumin signal peptide to secrete proteins in cells derived from different mammalian species. *Protein Expr Purif* **132**, 27–33 (2017).
67. Carofino, B. L., Ayanga, B. & Justice, M. J. A mouse model for inducible overexpression of Prdm14 results in rapid-onset and highly penetrant T-cell acute lymphoblastic leukemia (T-ALL). *DMM Disease Models and Mechanisms* **6**, 1494–1506 (2013).
68. Balnis, J. *et al.* Higher plasma levels of chemokine CCL19 are associated with poor SARS-CoV-2 acute respiratory distress syndrome (ARDS) outcomes. *medRxiv* (2020) doi:10.1101/2020.05.21.20051300.
69. Westermann, J. *et al.* CCL19 (ELC) as an adjuvant for DNA vaccination: induction of a TH1-type T-cell response and enhancement of antitumor immunity. *Cancer Gene Therapy 2007 14:6* **14**, 523–532 (2007).
70. Shabgah, A. G. *et al.* Does CCL19 act as a double-edged sword in cancer development? *Clin Exp Immunol* **207**, 164–175 (2022).
71. Wang, J. *et al.* CCL19 has potential to be a potential prognostic biomarker and a modulator of tumor immune microenvironment (TIME) of breast cancer: a comprehensive analysis based on TCGA database. *Aging (Albany NY)* **14**, 4158 (2022).
72. Damås, J. K. *et al.* Enhanced Expression of the Homeostatic Chemokines CCL19 and CCL21 in Clinical and Experimental Atherosclerosis. *Arterioscler Thromb Vasc Biol* **27**, 614–620 (2007).

Appendix I

pSUMO-mCCL19$_{(8-83)}$ GenBank data sequence.

LOCUS pSUMO-plasmid 5826 bp DNA circular SYN 13-JAN-2023

DEFINITION synthetic circular DNA.

KEYWORDS pSUMO-mCCL19_8-83

SOURCE synthetic DNA construct

ORGANISM synthetic DNA construct

REFERENCE 1 (bases 1 to 5826)

FEATURES Location/Qualifiers

source 1..5826

/mol_type="other DNA"

/organism="synthetic DNA construct"

terminator 26..73

/note="T7 terminator"

/note="transcription terminator for bacteriophage T7 RNA polymerase"

CDS complement(140..157)

/codon_start=1

/product="6xHis affinity tag"

/label=6xHis affinity tag

/note="6xHis"

/translation="HHHHHH"

CDS complement(203..430)

/codon_start=1

/product="mCCL198-83"

/label=mCCL19_8-83

/translation="CCLSVTQRPIPGNIVKAFRYLLNEDGCRVPAVVFTTLRGYQLCAP

PDQPWVDRIIRRLKKSSAKNKGNSTRRSPVS"

CDS complement(431..721)

/codon_start=1

/gene="S. cerevisiae SMT3 (truncated)"

/product="cleavable ubiquitin-like protein tag"

/label=S. cerevisiae SMT3 (truncated)

/note="SUMO"

/translation="SDSEVNQEAKPEVKPEVKPETHINLKVSDGSSEIFFKIKKTTPLR

RLMEAFAKRQGKEMDSLRFLYDGIRIQADQTPEDLDMEDNDIIEAHREQIGG"

CDS complement(725..742)

/codon_start=1

/product="6xHis affinity tag"

/label=6xHis affinity tag

/note="6xHis"

/translation="HHHHHH"

RBS 755..777

/note="efficient ribosome binding site from bacteriophage T7 gene 10 (Olins and Rangwala, 1989)"

protein_bind 792..816

/label=lac repressor encoded by lacI binding site

/bound_moiety="lac repressor encoded by lacI"

/note="lac operator"

/note="The lac repressor binds to the lac operator to inhibit transcription in E. coli. This inhibition can be relieved by adding lactose or isopropyl-beta-D-thiogalactopyranoside (IPTG)."

promoter complement(817..835)

/note="T7 promoter"

/note="promoter for bacteriophage T7 RNA polymerase"

promoter 1144..1221

/gene="lacI"

/label=lacI promoter

/note="lacI promoter"

CDS 1222..2304

/codon_start=1

/gene="lacI"

/product="lac repressor"

/label=lacI

/note="lacI"

/note="The lac repressor binds to the lac operator to
inhibit transcription in E. coli. This inhibition can be
relieved by adding lactose or
isopropyl-beta-D-thiogalactopyranoside (IPTG)."

/translation="MKPVTLYDVAEYAGVSYQTVSRVVNQASHVSAKTREKVEAAMAEL

NYIPNRVAQQLAGKQSLLIGVATSSLALHAPSQIVAAIKSRADQLGASVVVSMVERSGV

EACKAAVHNLLAQRVSGLIINYPLDDQDAIAVEAACTNVPALFLDVSDQTPINSIIFSH

EDGTRLGVEHLVALGHQQIALLAGPLSSVSARLRLAGWHKYLTRNQIQPIAEREGDWSA

MSGFQQTMQMLNEGIVPTAMLVANDQMALGAMRAITESGLRVGADISVVGYDDTEDS
SC

YIPPLTTIKQDFRLLGQTSVDRLLQLSQGQAVKGNQLLPVSLVKRKTTLAPNTQTASPR
ALADSLMQLARQVSRLESGQ"

CDS 3113..3304
/codon_start=1
/gene="rop"
/product="Rop protein, which maintains plasmids at low
copy number"

/label=rop

/note="rop"

/translation="MTKQEKTALNMARFIRSQTLTLLEKLNELDADEQADICESLHDHA
DELYRSCLARFGDDGENL"

misc_feature 3406..3548

/label=bom

/note="bom"

/note="basis of mobility region from pBR322"

rep_origin complement(3734..4322)

/direction=LEFT

/label=ori

/note="ori"

/note="high-copy-number ColE1/pMB1/pBR322/pUC origin of
replication"

CDS 4453..5268

/codon_start=1

/gene="aph(3')-Ia"

/product="aminoglycoside phosphotransferase"

/label=aph(3')-Ia

/note="KanR"

/note="confers resistance to kanamycin in bacteria or G418
(Geneticin(R)) in eukaryotes"

/translation="MSHIQRETSCSRPRLNSNMDADLYGYKWARDNVGQSGATIYRLYG

KPDAPELFLKHGKGSVANDVTDEMVRLNWLTEFMPLPTIKHFIRTPDDAWLLTTAIPGK

TAFQVLEEYPDSGENIVDALAVFLRRLHSIPVCNCPFNSDRVFRLAQAQSRMNNGLVDA

SDFDDERNGWPVEQVWKEMHKLLPFSPDSVVTHGDFSLDNLIFDEGKLIGCIDVGRVGI

ADRYQDLAILWNCLGEFSPSLQKRLFQKYGIDNPDMNKLQFHLMLDEFF"

rep_origin complement(5360..5815)

/direction=LEFT

/label=f1 ori

/note="f1 ori"

/note="f1 bacteriophage origin of replication; arrow

indicates direction of (+) strand synthesis"

ORIGIN

1 atccggatat agttcctcct ttcagcaaaa aacccctcaa gacccgttta gaggccccaa

61 ggggttatgc tagttattgc tcagcggtgg cagcagccaa ctcagcttcc tttcgggctt

121 tgttagcagc cggatctcag tggtggtggt ggtggtgctc gagtgcggcc gcaagcttgt

181 cgacggagct cgaattcgga tcgctaaccg gactacgacg ggtgctatta cctttgtttt

241 tggcgctgct ctttttcaga cgacgaataa tacgatcaac ccacggctga tcaggcggtg

301 cacacagctg ataaccacgc agtgtggtaa aaacaactgc cggaacacga caaccatctt

361 cgttcagcag ataacgaaat gctttaacaa tgttacccgg aatcggacgc tgggtaacgc

421 tcagacaaca acctccaatc tgttctctgt gagcctcaat aatatcgtta tcctccatgt

481 ccaaatcttc aggggtctga tcagcttgaa ttctaatacc gtcgtacaag aatcttaagg

541 agtccatttc cttaccctgt cttttagcga acgcttccat cagccttctt aaaggagtgg

601 tctttttgat cttgaagaag atctctgaag atccatcgga cacctttaaa ttgatgtgag

661 tctcaggctt gacttctggc ttgacctctg gcttagcttc ttgattgact tctgagtccg

721 acccgtgatg atgatggtga tgacccatgg tatatctcct tcttaaagtt aaacaaaatt

781 atttctagag gggaattgtt atccgctcac aattccccta tagtgagtcg tattaatttc

841 gcgggatcga gatctcgatc ctctacgccg gacgcatcgt ggccggcatc accggcgcca

901 caggtgcggt tgctggcgcc tatatcgccg acatcaccga tggggaagat cgggctcgcc

961 acttcgggct catgagcgct tgtttcggcg tgggtatggt ggcaggcccc gtggccgggg

1021 gactgttggg cgccatctcc ttgcatgcac cattccttgc ggcggcggtg ctcaacggcc

1081 tcaacctact actgggctgc ttcctaatgc aggagtcgca taagggagag cgtcgagatc

1141 ccggacacca tcgaatggcg caaaaccttt cgcggtatgg catgatagcg cccggaagag

1201 agtcaattca gggtggtgaa tgtgaaacca gtaacgttat acgatgtcgc agagtatgcc

1261 ggtgtctctt atcagaccgt ttcccgcgtg gtgaaccagg ccagccacgt ttctgcgaaa

1321 acgcgggaaa aagtggaagc ggcgatggcg gagctgaatt acattcccaa ccgcgtggca

1381 caacaactgg cgggcaaaca gtcgttgctg attggcgttg ccacctccag tctggccctg

1441 cacgcgccgt cgcaaattgt cgcggcgatt aaatctcgcg ccgatcaact gggtgccagc

1501 gtggtggtgt cgatggtaga acgaagcggc gtcgaagcct gtaaagcggc ggtgcacaat

1561 cttctcgcgc aacgcgtcag tgggctgatc attaactatc cgctggatga ccaggatgcc

1621 attgctgtgg aagctgcctg cactaatgtt ccggcgttat ttcttgatgt ctctgaccag

1681 acacccatca acagtattat tttctcccat gaagacggta cgcgactggg cgtggagcat

1741 ctggtcgcat tgggtcacca gcaaatcgcg ctgttagcgg gcccattaag ttctgtctcg

1801 gcgcgtctgc gtctggctgg ctggcataaa tatctcactc gcaatcaaat tcagccgata

1861 gcggaacggg aaggcgactg gagtgccatg tccggttttc aacaaaccat gcaaatgctg

1921 aatgagggca tcgttcccac tgcgatgctg gttgccaacg atcagatggc gctgggcgca

1981 atgcgcgcca ttaccgagtc cgggctgcgc gttggtgcgg atatctcggt agtgggatac

2041 gacgataccg aagacagctc atgttatatc ccgccgttaa ccaccatcaa acaggatttt

2101 cgcctgctgg ggcaaaccag cgtggaccgc ttgctgcaac tctctcaggg ccaggcggtg

2161 aagggcaatc agctgttgcc cgtctcactg gtgaaaagaa aaaccaccct ggcgcccaat

2221 acgcaaaccg cctctccccg cgcgttggcc gattcattaa tgcagctggc acgacaggtt

2281 tcccgactgg aaagcgggca gtgagcgcaa cgcaattaat gtaagttagc tcactcatta

2341 ggcaccggga tctcgaccga tgcccttgag agccttcaac ccagtcagct ccttccggtg

2401 ggcgcggggc atgactatcg tcgccgcact tatgactgtc ttctttatca tgcaactcgt

2461 aggacaggtg ccggcagcgc tctgggtcat tttcggcgag gaccgctttc gctggagcgc

2521 gacgatgatc ggcctgtcgc ttgcggtatt cggaatcttg cacgccctcg ctcaagcctt

2581 cgtcactggt cccgccacca aacgtttcgg cgagaagcag gccattatcg ccggcatggc

2641 ggccccacgg gtgcgcatga tcgtgctcct gtcgttgagg acccggctag gctggcgggg

2701 ttgccttact ggttagcaga atgaatcacc gatacgcgag cgaacgtgaa gcgactgctg

2761 ctgcaaaacg tctgcgacct gagcaacaac atgaatggtc ttcggtttcc gtgtttcgta

2821 aagtctggaa acgcggaagt cagcgccctg caccattatg ttccggatct gcatcgcagg

2881 atgctgctgg ctaccctgtg gaacacctac atctgtatta acgaagcgct ggcattgacc

2941 ctgagtgatt tttctctggt cccgccgcat ccataccgcc agttgtttac cctcacaacg

3001 ttccagtaac cgggcatgtt catcatcagt aacccgtatc gtgagcatcc tctctcgttt

3061 catcggtatc attaccccca tgaacagaaa tccccccttac acggaggcat cagtgaccaa

3121 acaggaaaaa accgccctta acatggcccg ctttatcaga agccagacat taacgcttct

3181 ggagaaactc aacgagctgg acgcggatga acaggcagac atctgtgaat cgcttcacga

3241 ccacgctgat gagctttacc gcagctgcct cgcgcgtttc ggtgatgacg gtgaaaacct

3301 ctgacacatg cagctcccgg agacggtcac agcttgtctg taagcggatg ccgggagcag

3361 acaagcccgt cagggcgcgt cagcgggtgt tggcgggtgt cggggcgcag ccatgaccca

3421 gtcacgtagc gatagcggag tgtatactgg cttaactatg cggcatcaga gcagattgta

3481 ctgagagtgc accatatatg cggtgtgaaa taccgcacag atgcgtaagg agaaaatacc

3541 gcatcaggcg ctcttccgct tcctcgctca ctgactcgct gcgctcggtc gttcggctgc

3601 ggcgagcggt atcagctcac tcaaaggcgg taatacggtt atccacagaa tcaggggata

3661 acgcaggaaa gaacatgtga gcaaaaggcc agcaaaaggc caggaaccgt aaaaaggccg

3721 cgttgctggc gtttttccat aggctccgcc cccctgacga gcatcacaaa aatcgacgct

3781 caagtcagag gtggcgaaac ccgacaggac tataaagata ccaggcgttt ccccctggaa

3841 gctccctcgt gcgctctcct gttccgaccc tgccgcttac cggatacctg tccgcctttc

3901 tcccttcggg aagcgtggcg ctttctcata gctcacgctg taggtatctc agttcggtgt

3961 aggtcgttcg ctccaagctg ggctgtgtgc acgaaccccc cgttcagccc gaccgctgcg

4021 ccttatccgg taactatcgt cttgagtcca acccggtaag acacgactta tcgccactgg

4081 cagcagccac tggtaacagg attagcagag cgaggtatgt aggcggtgct acagagttct

4141 tgaagtggtg gcctaactac ggctacacta gaaggacagt atttggtatc tgcgctctgc

4201 tgaagccagt taccttcgga aaaagagttg gtagctcttg atccggcaaa caaaccaccg

4261 ctggtagcgg tggtttttt gtttgcaagc agcagattac gcgcagaaaa aaaggatctc

4321 aaagctgtat cgaagatcct ttgatctttt ctacggggtc tgacgctcag tggaacgaaa

4381 actcacgtta agggattttg gtcatgaaca ataaaactgt ctgcttacat aaacagtaat

4441 acaaggggtg ttatgagcca tattcaacgg gaaacgtctt gctctaggcc gcgattaaat

4501 tccaacatgg atgctgattt atatgggtat aaatgggctc gcgataatgt cgggcaatca

4561 ggtgcgacaa tctatcgatt gtatgggaag cccgatgcgc cagagttgtt tctgaaacat

4621 ggcaaaggta gcgttgccaa tgatgttaca gatgagatgg tcagactaaa ctggctgacg

4681 gaatttatgc ctcttccgac catcaagcat tttatccgta ctcctgatga tgcatggtta

4741 ctcaccactg cgatccccgg gaaaacagca ttccaggtat tagaagaata tcctgattca

4801 ggtgaaaata ttgttgatgc gctggcagtg ttcctgcgcc ggttgcattc gattcctgtt

4861 tgtaattgtc cttttaacag cgatcgcgta tttcgtctcg ctcaggcgca atcacgaatg

4921 aataacggtt tggttgatgc gagtgatttt gatgacgagc gtaatggctg gcctgttgaa

4981 caagtctgga aagaaatgca taaacttttg ccattctcac cggattcagt cgtcactcat

5041 ggtgatttct cacttgataa ccttatttttt gacgagggga aattaatagg ttgtattgat

5101 gttggacgag tcggaatcgc agaccgatac caggatcttg ccatcctatg gaactgcctc

5161 ggtgagtttt ctccttcatt acagaaacgg ctttttcaaa aatatggtat tgataatcct

5221 gatatgaata aattgcagtt tcatttgatg ctcgatgagt ttttctaaga attaattcat

5281 gagcggatac atatttgaat gtatttagaa aaataaacaa ataggggttc cgcgcacatt

5341 tccccgaaaa gtgccaccta aattgtaagc gttaatattt tgttaaaatt cgcgttaaat

5401 ttttgttaaa tcagctcatt ttttaaccaa taggccgaaa tcggcaaaat cccttataaa

5461 tcaaaagaat agaccgagat agggttgagt gttgttccag tttggaacaa gagtccacta

5521 ttaaagaacg tggactccaa cgtcaaaggg cgaaaaaccg tctatcaggg cgatggccca

5581 ctacgtgaac catcacccta atcaagtttt ttggggtcga ggtgccgtaa agcactaaat

5641 cggaacccta aagggagccc ccgatttaga gcttgacggg gaaagccggc gaacgtggcg

5701 agaaaggaag ggaagaaagc gaaaggagcg ggcgctaggg cgctggcaag tgtagcggtc

5761 acgctgcgcg taaccaccac acccgccgcg cttaatgcgc cgctacaggg cgcgtcccat

5821 tcgcca

Appendix II

pcDNA 3.1 (+) IgkH-8His-SMT3-CCL19$_{(8\text{-}83)}$ GenBank Data Sequence.

LOCUS 22ABMDBD_IgkH-His-SMT3-CCL883_pcDNA3.1(+) 5987 bp DNA circular 31-JUL-2014

FEATURES Location/Qualifiers

promoter 863..881
/label="T7_promoter"

promoter complement(5893..5921)
/label="AmpR_promoter"

promoter 2429..2631
/label="SV40_promoter"

terminator 1581..1808
/label="bGH_PA_terminator"

CDS complement(4991..5851)
/label="Amp(R)"

CDS 2683..3483
/label="Neo(R)"

rep_origin complement(4217..4836)
/label="pBR322_origin"

rep_origin 2476..2553
/label="SV40_origin"

rep_origin 1871..2177
/label="f1_origin"

primer complement(3826..3844)

/label="M13_reverse_primer"

primer complement(1578..1595)

/label="BGH\rev\primer"

primer 769..789

/label="CMV_fwd_primer"

primer 3751..3770

/label="EBV_rev_primer"

primer complement(3843..3865)

/label="M13_pUC_rev_primer"

primer complement(2291..2311)

/label="pBABE_3_primer"

primer 2538..2557

/label="SV40pro_F_primer"

polyA_site 1584..1808

/label="BGH\pA"

promoter 308..818

/label="CMV_Promoter"

terminator 3665..3781

/label="SV40_PA_terminator"

promoter 236..852

/label="CMV_immearly_promoter"

CDS 2692..3486

/label="Neo_Kana"

gene 929..1546

/label="IgkH-His-SMT3-CCL883"

ORIGIN

1 GACGGATCGG GAGATCTCCC GATCCCCTAT GGTGCACTCT CAGTACAATC TGCTCTGATG

61 CCGCATAGTT AAGCCAGTAT CTGCTCCCTG CTTGTGTGTT GGAGGTCGCT GAGTAGTGCG

121 CGAGCAAAAT TTAAGCTACA ACAAGGCAAG GCTTGACCGA CAATTGCATG AAGAATCTGC

181 TTAGGGTTAG GCGTTTTGCG CTGCTTCGCG ATGTACGGGC CAGATATACG CGTTGACATT

241 GATTATTGAC TAGTTATTAA TAGTAATCAA TTACGGGGTC ATTAGTTCAT AGCCCATATA

301 TGGAGTTCCG CGTTACATAA CTTACGGTAA ATGGCCCGCC TGGCTGACCG CCCAACGACC

361 CCCGCCCATT GACGTCAATA ATGACGTATG TTCCCATAGT AACGCCAATA GGGACTTTCC

421 ATTGACGTCA ATGGGTGGAG TATTTACGGT AAACTGCCCA CTTGGCAGTA CATCAAGTGT

481 ATCATATGCC AAGTACGCCC CCTATTGACG TCAATGACGG TAAATGGCCC GCCTGGCATT

541 ATGCCCAGTA CATGACCTTA TGGGACTTTC CTACTTGGCA GTACATCTAC GTATTAGTCA

601 TCGCTATTAC CATGGTGATG CGGTTTTGGC AGTACATCAA TGGGCGTGGA TAGCGGTTTG

661 ACTCACGGGG ATTTCCAAGT CTCCACCCCA TTGACGTCAA TGGGAGTTTG TTTTGGCACC

721 AAAATCAACG GGACTTTCCA AAATGTCGTA ACAACTCCGC CCCATTGACG CAAATGGGCG

781 GTAGGCGTGT ACGGTGGGAG GTCTATATAA GCAGAGCTCT CTGGCTAACT AGAGAACCCA

841 CTGCTTACTG GCTTATCGAA ATTAATACGA CTCACTATAG GGAGACCCAA GCTGGCTAGC

901 GTTTAAACTT AAGCTTGGTA CCGAGCTCGG ATCCATGGAA GCTCCTGCTC AGCTGCTGTT

961 CCTGCTGCTG CTGTGGCTGC CTGATACCAC AGGACACCAC CATCATCACC ATCACCACAG

1021 CGACAGCGAA GTGAATCAAG AGGCCAAGCC TGAAGTGAAA CCCGAAGTGA AGCCTGAGAC

1081 ACACATCAAC CTGAAGGTGT CCGACGGCAG CAGCGAGATC TTCTTCAAGA TCAAGAAAAC

1141 CACACCTCTG CGGCGGCTGA TGGAAGCCTT CGCCAAAAGA CAGGGCAAAG AGATGGACAG

1201 CCTGCGGTTC CTGTACGACG GCATCAGAAT CCAGGCCGAT CAGACCCCTG AGGACCTGGA

1261 CATGGAAGAT AACGACATCA TCGAGGCCCA CAGAGAGCAG ATCGGCGGCT GTTGTCTGAG

1321 CGTGACCCAG AGGCCTATTC CTGGCAACAT CGTGAAGGCC TTTCGCTACC TGCTGAACGA

1381 GGACGGCTGT AGAGTGCCTG CCGTGGTGTT CACAACCCTG AGAGGCTACC AGCTGTGCGC

1441 CCCTCCTGAT CAACCTTGGG TCGACCGGAT CATCAGACGG CTGAAGAAGT CCAGCGCCAA

1501 GAACAAGGGC AACAGCACTA GACGCAGCCC CGTGTCTTAA CTCGAGTCTA GAGGGCCCGT

1561 TTAAACCCGC TGATCAGCCT CGACTGTGCC TTCTAGTTGC CAGCCATCTG TTGTTTGCCC

1621 CTCCCCCGTG CCTTCCTTGA CCCTGGAAGG TGCCACTCCC ACTGTCCTTT CCTAATAAAA

1681 TGAGGAAATT GCATCGCATT GTCTGAGTAG GTGTCATTCT ATTCTGGGGG GTGGGGTGGG

1741 GCAGGACAGC AAGGGGGAGG ATTGGGAAGA CAATAGCAGG CATGCTGGGG ATGCGGTGGG

1801 CTCTATGGCT TCTGAGGCGG AAAGAACCAG CTGGGGCTCT AGGGGGTATC CCCACGCGCC

1861 CTGTAGCGGC GCATTAAGCG CGGCGGGTGT GGTGGTTACG CGCAGCGTGA CCGCTACACT

1921 TGCCAGCGCC CTAGCGCCCG CTCCTTTCGC TTTCTTCCCT TCCTTTCTCG CCACGTTCGC

1981 CGGCTTTCCC CGTCAAGCTC TAAATCGGGG GCTCCCTTTA GGGTTCCGAT TTAGTGCTTT

2041 ACGGCACCTC GACCCCAAAA AACTTGATTA GGGTGATGGT TCACGTAGTG GGCCATCGCC

2101 CTGATAGACG GTTTTTCGCC CTTTGACGTT GGAGTCCACG TTCTTTAATA GTGGACTCTT

2161 GTTCCAAACT GGAACAACAC TCAACCCTAT CTCGGTCTAT TCTTTTGATT TATAAGGGAT

2221 TTTGCCGATT TCGGCCTATT GGTTAAAAAA TGAGCTGATT TAACAAAAAT TTAACGCGAA

2281 TTAATTCTGT GGAATGTGTG TCAGTTAGGG TGTGGAAAGT CCCCAGGCTC CCCAGCAGGC

2341 AGAAGTATGC AAAGCATGCA TCTCAATTAG TCAGCAACCA GGTGTGGAAA GTCCCCAGGC

2401 TCCCCAGCAG GCAGAAGTAT GCAAAGCATG CATCTCAATT AGTCAGCAAC CATAGTCCCG

2461 CCCCTAACTC CGCCCATCCC GCCCCTAACT CCGCCCAGTT CCGCCCATTC TCCGCCCCAT

2521 GGCTGACTAA TTTTTTTTAT TTATGCAGAG GCCGAGGCCG CCTCTGCCTC TGAGCTATTC

2581 CAGAAGTAGT GAGGAGGCTT TTTTGGAGGC CTAGGCTTTT GCAAAAAGCT CCCGGGAGCT

2641 TGTATATCCA TTTTCGGATC TGATCAAGAG ACAGGATGAG GATCGTTTCG CATGATTGAA

2701 CAAGATGGAT TGCACGCAGG TTCTCCGGCC GCTTGGGTGG AGAGGCTATT CGGCTATGAC

2761 TGGGCACAAC AGACAATCGG CTGCTCTGAT GCCGCCGTGT TCCGGCTGTC AGCGCAGGGG

2821 CGCCCGGTTC TTTTTGTCAA GACCGACCTG TCCGGTGCCC TGAATGAACT GCAGGACGAG

2881 GCAGCGCGGC TATCGTGGCT GGCCACGACG GGCGTTCCTT GCGCAGCTGT GCTCGACGTT

2941 GTCACTGAAG CGGGAAGGGA CTGGCTGCTA TTGGGCGAAG TGCCGGGGCA GGATCTCCTG

3001 TCATCTCACC TTGCTCCTGC CGAGAAAGTA TCCATCATGG CTGATGCAAT GCGGCGGCTG

3061 CATACGCTTG ATCCGGCTAC CTGCCCATTC GACCACCAAG CGAAACATCG CATCGAGCGA

3121 GCACGTACTC GGATGGAAGC CGGTCTTGTC GATCAGGATG ATCTGGACGA AGAGCATCAG

3181 GGGCTCGCGC CAGCCGAACT GTTCGCCAGG CTCAAGGCGC GCATGCCCGA CGGCGAGGAT

3241 CTCGTCGTGA CCCATGGCGA TGCCTGCTTG CCGAATATCA TGGTGGAAAA TGGCCGCTTT

3301 TCTGGATTCA TCGACTGTGG CCGGCTGGGT GTGGCGGACC GCTATCAGGA CATAGCGTTG

3361 GCTACCCGTG ATATTGCTGA AGAGCTTGGC GGCGAATGGG CTGACCGCTT CCTCGTGCTT

3421 TACGGTATCG CCGCTCCCGA TTCGCAGCGC ATCGCCTTCT ATCGCCTTCT TGACGAGTTC

3481 TTCTGAGCGG GACTCTGGGG TTCGAAATGA CCGACCAAGC GACGCCCAAC CTGCCATCAC

3541 GAGATTTCGA TTCCACCGCC GCCTTCTATG AAAGGTTGGG CTTCGGAATC GTTTTCCGGG

3601 ACGCCGGCTG GATGATCCTC CAGCGCGGGG ATCTCATGCT GGAGTTCTTC GCCCACCCCA

3661 ACTTGTTTAT TGCAGCTTAT AATGGTTACA AATAAAGCAA TAGCATCACA AATTTCACAA

3721 ATAAAGCATT TTTTTCACTG CATTCTAGTT GTGGTTTGTC CAAACTCATC AATGTATCTT

3781 ATCATGTCTG TATACCGTCG ACCTCTAGCT AGAGCTTGGC GTAATCATGG TCATAGCTGT

3841 TTCCTGTGTG AAATTGTTAT CCGCTCACAA TTCCACACAA CATACGAGCC GGAAGCATAA

3901 AGTGTAAAGC CTGGGGTGCC TAATGAGTGA GCTAACTCAC ATTAATTGCG TTGCGCTCAC

3961 TGCCCGCTTT CCAGTCGGGA AACCTGTCGT GCCAGCTGCA TTAATGAATC GGCCAACGCG

4021 CGGGGAGAGG CGGTTTGCGT ATTGGGCGCT CTTCCGCTTC CTCGCTCACT GACTCGCTGC

4081 GCTCGGTCGT TCGGCTGCGG CGAGCGGTAT CAGCTCACTC AAAGGCGGTA ATACGGTTAT

4141 CCACAGAATC AGGGGATAAC GCAGGAAAGA ACATGTGAGC AAAAGGCCAG CAAAAGGCCA

4201 GGAACCGTAA AAAGGCCGCG TTGCTGGCGT TTTTCCATAG GCTCCGCCCC CCTGACGAGC

4261 ATCACAAAAA TCGACGCTCA AGTCAGAGGT GGCGAAACCC GACAGGACTA TAAAGATACC

4321 AGGCGTTTCC CCCTGGAAGC TCCCTCGTGC GCTCTCCTGT TCCGACCCTG CCGCTTACCG

4381 GATACCTGTC CGCCTTTCTC CCTTCGGGAA GCGTGGCGCT TTCTCATAGC TCACGCTGTA

4441 GGTATCTCAG TTCGGTGTAG GTCGTTCGCT CCAAGCTGGG CTGTGTGCAC GAACCCCCCG

4501 TTCAGCCCGA CCGCTGCGCC TTATCCGGTA ACTATCGTCT TGAGTCCAAC CCGGTAAGAC

4561 ACGACTTATC GCCACTGGCA GCAGCCACTG GTAACAGGAT TAGCAGAGCG AGGTATGTAG

4621 GCGGTGCTAC AGAGTTCTTG AAGTGGTGGC CTAACTACGG CTACACTAGA AGAACAGTAT

4681 TTGGTATCTG CGCTCTGCTG AAGCCAGTTA CCTTCGGAAA AAGAGTTGGT AGCTCTTGAT

4741 CCGGCAAACA AACCACCGCT GGTAGCGGTG GTTTTTTTGT TTGCAAGCAG CAGATTACGC

4801 GCAGAAAAAA AGGATCTCAA GAAGATCCTT TGATCTTTTC TACGGGGTCT GACGCTCAGT

4861 GGAACGAAAA CTCACGTTAA GGGATTTTGG TCATGAGATT ATCAAAAAGG ATCTTCACCT

4921 AGATCCTTTT AAATTAAAAA TGAAGTTTTA AATCAATCTA AAGTATATAT GAGTAAACTT

4981 GGTCTGACAG TTACCAATGC TTAATCAGTG AGGCACCTAT CTCAGCGATC TGTCTATTTC

5041 GTTCATCCAT AGTTGCCTGA CTCCCCGTCG TGTAGATAAC TACGATACGG GAGGGCTTAC

5101 CATCTGGCCC CAGTGCTGCA ATGATACCGC GAGACCCACG CTCACCGGCT CCAGATTTAT

5161 CAGCAATAAA CCAGCCAGCC GGAAGGGCCG AGCGCAGAAG TGGTCCTGCA ACTTTATCCG

5221 CCTCCATCCA GTCTATTAAT TGTTGCCGGG AAGCTAGAGT AAGTAGTTCG CCAGTTAATA

5281 GTTTGCGCAA CGTTGTTGCC ATTGCTACAG GCATCGTGGT GTCACGCTCG TCGTTTGGTA

5341 TGGCTTCATT CAGCTCCGGT TCCCAACGAT CAAGGCGAGT TACATGATCC CCCATGTTGT

5401 GCAAAAAAGC GGTTAGCTCC TTCGGTCCTC CGATCGTTGT CAGAAGTAAG TTGGCCGCAG

5461 TGTTATCACT CATGGTTATG GCAGCACTGC ATAATTCTCT TACTGTCATG CCATCCGTAA

5521 GATGCTTTTC TGTGACTGGT GAGTACTCAA CCAAGTCATT CTGAGAATAG TGTATGCGGC

5581 GACCGAGTTG CTCTTGCCCG GCGTCAATAC GGGATAATAC CGCGCCACAT AGCAGAACTT

5641 TAAAAGTGCT CATCATTGGA AAACGTTCTT CGGGGCGAAA ACTCTCAAGG ATCTTACCGC

5701 TGTTGAGATC CAGTTCGATG TAACCCACTC GTGCACCCAA CTGATCTTCA GCATCTTTTA

5761 CTTTCACCAG CGTTTCTGGG TGAGCAAAAA CAGGAAGGCA AAATGCCGCA AAAAAGGGAA

5821 TAAGGGCGAC ACGGAAATGT TGAATACTCA TACTCTTCCT TTTTCAATAT TATTGAAGCA

5881 TTTATCAGGG TTATTGTCTC ATGAGCGGAT ACATATTTGA ATGTATTTAG AAAAATAAAC

5941 AAATAGGGGT TCCGCGCACA TTTCCCCGAA AAGTGCCACC TGACGTC

//

Curriculum Vita

Angel Torres received his Bachelor of Science degree in Microbiology from The University of Texas at El Paso in 2018. In Fall 2019, he joined the master program in Bioscience in the Department of Biological Sciences at The University of Texas at El Paso, where he joined Dr. Charlotte M. Vines laboratory and began his research in protein purification.

Mr. Torres during his time at UTEP would lecture undergraduates in a Research Driven Courses (RDCs) under the Freshman Year Research Intensive Sequence (FYRIS) program, funded by the National Institute of Health (NIH) – Building Infrastructure Leading Diversity Southwest Consortium of Health-Oriented Education Leaders and Research Scholars (BUILD SCHOLARS). Allowing entering first-year students to gain real-world research experience in a field of interest related to their majors while producing useful data for their professor's research project.

While pursuing his master's degree, Mr. Torres attended and presented a poster at The American Association for Cancer Research (AACR) in New Orleans 2022. He remained active and further progressed his career by obtaining a position working in the Biomolecule Analysis and Omics Unit (BAOU) at the Border Biomedical Research Center.

Mr. Torres thesis was supervised by Dr. Charlotte M. Vines. Upon graduation, Mr. Torres plans to pursue a career in biotechnology.

Contact Information: atorres61@miners.utep.edu